PLOS ONE

RESEARCH ARTICLE

The Advanced BRain Imaging on ageing and Memory (ABRIM) data collection: Study design, data processing, and rationale

Michelle G. Jansen[1], Marcel P. Zwiers[2], Jose P. Marques[2], Kwok-Shing Chan[2], Jitse S. Amelink[2,3], Mareike Altgassen[4], Joukje M. Oosterman[1☯*], David G. Norris[2☯]

1 Donders Centre for Cognition, Donders Institute for Brain, Cognition and Behaviour, Radboud University, Nijmegen, the Netherlands, **2** Donders Centre for Cognitive Neuroimaging, Donders Institute for Brain, Cognition and Behaviour, Radboud University, Nijmegen, the Netherlands, **3** Language and Genetics Department, Max Planck Institute for Psycholinguistics, Radboud University, Nijmegen, the Netherlands, **4** Department of Psychology, Johannes Gutenberg-University Mainz, Mainz, Germany

☯ These authors contributed equally to this work.
* joukje.oosterman@donders.ru.nl

Citation: Jansen MG, Zwiers MP, Marques JP, Chan K-S, Amelink JS, Altgassen M, et al. (2024) The Advanced BRain Imaging on ageing and Memory (ABRIM) data collection: Study design, data processing, and rationale. PLoS ONE 19(6): e0306006. https://doi.org/10.1371/journal.pone.0306006

Editor: Md Nasir Uddin, University of Rochester, UNITED STATES

Received: January 16, 2024

Accepted: June 7, 2024

Published: June 21, 2024

Data Availability Statement: Data required to replicate the results presented in this study are available via: https://doi.org/10.34973/jyeh-kp46.

Funding: The study was funded by the European FP7 program, FP7-PEOPLE-2013-ITN, Marie-Curie Action, "Initial Training Networks" named "Advanced Brain Imaging with MRI" (no. 608123). The funders had no role in study design, data collection and analysis, decision to publish, or preparation of the manuscript.

Abstract

To understand the neurocognitive mechanisms that underlie heterogeneity in cognitive ageing, recent scientific efforts have led to a growing public availability of imaging cohort data. The Advanced BRain Imaging on ageing and Memory (ABRIM) project aims to add to these existing datasets by taking an adult lifespan approach to provide a cross-sectional, normative database with a particular focus on connectivity, myelinization and iron content of the brain in concurrence with cognitive functioning, mechanisms of reserve, and sleep-wake rhythms. ABRIM freely shares MRI and behavioural data from 295 participants between 18–80 years, stratified by age decade and sex (median age 52, IQR 36–66, 53.20% females). The ABRIM MRI collection consists of both the raw and pre-processed structural and functional MRI data to facilitate data usage among both expert and non-expert users. The ABRIM behavioural collection includes measures of cognitive functioning (i.e., global cognition, processing speed, executive functions, and memory), proxy measures of cognitive reserve (e.g., educational attainment, verbal intelligence, and occupational complexity), and various self-reported questionnaires (e.g., on depressive symptoms, pain, and the use of memory strategies in daily life and during a memory task). In a sub-sample ($n = 120$), we recorded sleep-wake rhythms using an actigraphy device (Actiwatch 2, Philips Respironics) for a period of 7 consecutive days. Here, we provide an in-depth description of our study protocol, pre-processing pipelines, and data availability. ABRIM provides a cross-sectional database on healthy participants throughout the adult lifespan, including numerous parameters relevant to improve our understanding of cognitive ageing. Therefore, ABRIM enables researchers to model the advanced imaging parameters and cognitive topologies as a function of age, identify the normal range of values of such parameters, and to further investigate the diverse mechanisms of reserve and resilience.

Competing interests: The authors have declared that no competing interests exist.

Introduction

Due to the worldwide ageing of the population, the proportion of adults who are suffering from or are at risk of cognitive impairment increases. This emphasizes the need to understand the building blocks of healthy cognitive ageing to reduce or even mitigate the decline in cognition that is associated with ageing [1, 2]. Normal ageing is accompanied by heterogeneous trajectories of cognitive decline within and across individuals, and predominantly affects processing speed, episodic memory, and reasoning [3, 4]. Where some individuals maintain a high level of cognitive functioning even throughout advanced age, others experience cognitive deficits that profoundly impact their daily lives [5, 6].

A growing body of research therefore seeks to explain individual variability in cognitive ageing by focusing on the underlying neural mechanisms [6, 7]. Brain ageing features that have been associated with lower cognitive functioning include a loss of brain volume and cortical thinning [8, 9], alterations in microstructural integrity, white matter organization, and cortical myelination [10–12], accumulation of iron content [13], and alterations in resting-state functional connectivity [14, 15]. However, patterns of brain ageing are highly variable across individuals, and marked differences exist in the extent of age-related brain changes as well as in the regional specificity of such alterations [16–18]. The concurrent investigation of brain ageing metrics therefore could provide complementary information on brain-cognition dynamics in ageing [18, 19].

Another approach to study heterogeneity in cognitive ageing involves identifying the factors that contribute to risk or resilience [2, 6, 17, 20]. Factors such as hypertension, diabetes, obesity, physical inactivity, sleep disturbances, and depressive symptoms contribute to an increased risk of cognitive decline [2, 20]. In contrast, protective factors include, for example, educational attainment, occupational complexity, engagement in mentally stimulating activities, and social engagement [2, 17, 20]. It is assumed that risk factors of cognitive decline impact cognitive abilities through their associations with decreased brain health [21, 22]. However, it remains to be elucidated whether protective factors promote cognition through neuroprotective effects (i.e., brain maintenance), stable neural advantages (i.e., brain reserve), and/or moderate the effects of neurodegeneration on cognition (i.e., cognitive reserve, CR) [6, 17, 23, 24]. As brain health measures only partially explain heterogeneity in cognitive functioning, further insights on the precise working mechanisms of these protective factors are especially important [25].

Taken together, an extensive characterization of brain health parameters together with other factors of risk and resilience in cognitive ageing is warranted to increase our understanding of differing trajectories in ageing. Consequently, increasing efforts are made to facilitate the public availability of large neuroimaging datasets, directly via online repositories [26–29], or upon request and/or application [30–34].

The Advanced BRain Imaging on ageing and Memory (ABRIM) project aims to add to these existing datasets in several ways. First, only a few databases cover the adult lifespan [28, 31], whereas it is critical to map cognitive performance and brain health across all age groups. We therefore collected a cross-sectional, normative database of adults between 18–80 years old, stratified by age decade and sex. Second, quantitative imaging techniques are scarcely available in large population studies [26, 28, 33]. Quantitative imaging is particularly useful to investigate myelination and iron depositions in the brain [35–37], and has been associated with cognitive performance in normal aging [13, 38]. Our neuroimaging protocol therefore not only matches the sequences of the aforementioned datasets (i.e., conventional structural T1- and T2-weighted imaging, multi-shell diffusion weighted imaging, and resting-state functional MRI), but also facilitates quantitative imaging with Magnetization Prepared 2 RApid

Gradient Echoes (MP2RAGE) and Multi Echo Gradient Echo Imaging (MEGRE) sequences. Where MP2RAGE allows to compute longitudinal relaxation rates (R_1 = 1/T1), MEGRE allows to derive apparent transverse relaxation rates (R_2^*) and quantitative susceptibility maps (QSM) [39, 40]. Lastly, in addition to cognitive test performance, we measured several variables associated with risk or resilience in cognitive ageing with self-reported questionnaires (e.g., on depressive symptoms and memory strategy use), a semi-structured interview (e.g., on educational attainment, occupational complexity, and leisure activities), and actigraphy (for sleep and physical activity estimates). This allows us to map the interactions of these variables with brain health across the lifespan more comprehensively. A complete overview of the variables that are included in ABRIM, in addition to the aforementioned neuroimaging datasets, is provided in S1 Table.

Below, we outline the study protocol of ABRIM, participant inclusion and exclusion procedures, behavioural and cognitive assessment, MRI sequences, and pre-processing pipelines. Furthermore, we describe our data sharing and management policies, as guided by the FAIR (Findable, Accessible, Interoperable, and Reusable) principles [41]. ABRIM makes it possible to model imaging parameters and cognitive topologies throughout the adult lifespan, identify the normal range of values of such parameters, and further investigate the mechanisms that contribute to cognitive performance across the adult lifespan.

Materials and methods

Participants

The study was performed at the Donders Institute for Brain, Cognition, and Behaviour, Radboud University Nijmegen the Netherlands. Recruitment of participants occurred between February 2017 and May 2022. The present study focused on a healthy, adult lifespan sample (18–80 years old).

We aimed to include approximately 25 male and 25 female participants per approximate age decade of adult life (18–30, 31–40, 41–50, 51–60, 61–70, 71–80). We recruited 301 participants from the general population, predominantly from the Nijmegen area. Several methods were employed to facilitate recruitment, including online and offline advertisements (e.g., on social media or in local supermarkets) and word of mouth. Participants were provided with a reimbursement of 10 euros per hour per bank transfer.

Potential participants were screened for inclusion via telephone or e-mail with a standardized questionnaire. Exclusion criteria consisted of the presence of any conditions with a profound impact on the brain and cognitive health, beyond normal aging, including current psychiatric disorders (e.g., major depressive disorder, bipolar disorder, schizophrenia), neurological conditions (e.g., dementia, history of stroke, epilepsy), substance use disorders (e.g., addiction to hard drugs), and history of other major health conditions that could impact cognition (e.g., history of brain tumour). Participants were additionally excluded if any MRI contraindications were present (e.g., ferromagnetic metal implants, claustrophobia, pregnancy).

It should be noted that an additional n = 108 participants were recruited prior to the start of the MRI acquisition, which was delayed due to a scanner upgrade. However, once the MRI acquisition was started (approximately 4–6 months after initial inclusion), these participants did not undergo the MRI protocol due to various reasons (e.g., no answer, lack of interest, unavailability, or MRI contraindications that were not previously mentioned). To ensure that our final MRI study sample included approximately 300 participants, we extended our recruitment.

Ethical approval

The entire study was conducted in compliance with the Helsinki declaration. The study fell under the blanket ethics approval "Image Human Cognition" (Commissie Mensgebonden Onderzoek Arnhem-Nijmegen, 2014/288), and was additionally approved by the Social Sciences Ethical Committee of the Radboud University (ECSW 2017-3001-46) and was conducted in compliance with all local procedures and applicable national legislation. All participants provided written informed consent prior to participation.

Data management

We follow the requirements of the European General Data Protection Regulation (GDPR; https://gdpr.eu/) and the Dutch Act on Implementation of the General Data Protection Regulation.

To ensure anonymity of participants, privacy sensitive participant information (i.e., personal data) was separately stored in a password-protected database and only accessible to the main investigators. Participant data (i.e., scientific data) was anonymized and stored using study-specific numerical identification codes. A separate password-protected key file, that serves just to link participant identification codes to participant's names, was kept by one researcher in strict confidence. We destroyed all privacy sensitive information and the key file one year after study completion, unless permission was granted by participants to be contacted in the future to be asked to participate in other studies. Signed informed consents and screening forms were locally archived in a closed locker at the Donders Institute, Nijmegen, the Netherlands, for at least 15 years after study completion. The original documents from the behavioural and cognitive examination (e.g., paper-and-pencil tests, self-reported questionnaires) were archived in a similar manner.

During data acquisition and analysis, raw actigraphy data was stored on a network directory from the Radboud University, Nijmegen, the Netherlands. With regards to MRI data, data were stored in a similarly secured way on network directory at the Donders Institute. Data storage is provided for by the main investigators of the study (MJ, JMO, DGN) and is accessible only for researchers involved in the processing of ABRIM.

With regards to data management of demographic variables and outcome measures of neuropsychological tests, self-reported questionnaires, and actigraphy, we used Castor (https://www.castoredc.com/). Castor provides a secured, cloud-based platform that supports researchers with adhering to Good Clinical Practice (GCP) guidelines (e.g., by saving all entered data and any changes that are being made). The study data is archived in Castor for 15 years for traceability purposes in accordance with GCP. All data stored in Castor is available for researchers involved in processing of the study after access has been granted by the main investigators.

For archiving purposes, raw DICOM MRI images, raw actigraphy data, and the Castor export were transferred to the Radboud Data Repository (https://data.ru.nl/). All research data is archived for at least 10 years after study completion.

Notably, the Radboud Data Repository consists of non-shared data collections for archiving purposes (i.e., data acquisition collection, DAC), as well as shared data collections of pre-processed or anonymized data (i.e., data sharing collection, DSC).

ABRIM data sharing is facilitated through the Radboud Data Repository, with one DSC for the neuroimaging data (ABRIM MRI collection) and a second DSC for the cognitive and behavioural data (ABRIM behavioural collection). A complete description of the included measures in both data sharing collections are provided below. To facilitate data sharing and ensure pseudonymization, data were stored using non-identifiable codes, data were minimized as much as

possible (e.g., no birth data, only age), and all anatomical scans were defaced prior to further processing (see "Methods" for details).

All data sharing procedures are in accordance with the agreements specified in the participants' signed informed consent, and in consultation with the local privacy officer to ensure compliance to the relevant regulations, sharing as openly as possible but as restricted as needed due to privacy legislation.

Cognitive and behavioural data

Cognitive and behavioural examination. The cognitive and behavioural examinations were performed by trained researchers and consisted of a neuropsychological assessment, several self-report questionnaires, and a semi-structured interview to evaluate cognitive reserve.

The complete assessment took up to 2 hours and was performed in a quiet office-like environment without any distractions. Due to participant availability and logistics, not all assessments were performed on the same day as the MRI protocol (median days between assessments = 0, IQR 0–33.75). The order of the protocol was fixed to ensure that during the delay intervals for each memory test no new verbal stimuli to memorize were introduced. Below, we provide a detailed description of the different procedures and measures that were obtained. Notably, ongoing efforts to improve the cognitive and behavioural assessment introduced several novel components to the protocol throughout the course of the study, as indicated below.

Demographics, general health, and lifestyle variables. Standardized, self-report questionnaires were used to obtain information on demographics (age, sex, highest level of completed education), relevant medical conditions (e.g., hypertension, rheumatism), use of medication, and lifestyle habits (e.g., smoking behaviour, use of alcoholic beverages).

We used the International Standard Classification of Education (ISCED-11 [42]) to classify educational attainment into three levels: low education (early childhood, primary, and lower secondary education; ISCED 0–2), medium education (upper secondary and post-secondary non-tertiary education; ISCED 3–4), high education (short cycle tertiary education, bachelor, master, and doctoral or equivalent education, ISCED 5–8).

With regards to relevant medical conditions, participants were asked to report any current or previous psychiatric or neurological conditions, substance abuse, cerebrovascular accidents, cardiovascular disease, rheumatism, hypertension, hypercholesteremia, diabetes, sleep disorders, and chronic pain conditions. We evaluated the presence of these conditions not only to ensure compliance with the inclusion criteria, but also to inform on several, frequently occurring age-related conditions that did not warrant exclusion for the present study (e.g., rheumatism, hypertension, hypercholesteremia, diabetes, sleep disorders, chronic pain). In addition, participants were asked to rate their current and monthly pain using a numerical rating scale ranging between 0 (no pain) and 10 (worst pain imaginable).

Furthermore, participants were asked to provide a list of their current medication use. Subsequently, we classified them into the following categories: 1) psychoactive medication (e.g., antidepressants or antipsychotics); 2) tranquilizers or sleep medication (e.g., benzodiazepines); 3) anticoagulants (e.g., heparin); 4) antiplatelets (e.g., acetylsalicylic acid); 5) blood pressure medication (e.g., diuretics); 6) cholesterol medication (e.g., statins); and 7) diabetes medication (e.g., insulin).

We incorporated a customized, self-report questionnaire to the study after data were collected for ±100 participants to obtain information on smoking behaviour (current, ever smoking, or no smoking) and use of alcoholic beverages, in terms of average drinking frequency (never, monthly or less, 2–4 times a month, 2–3 times per week, 4 or more times per week),

average number of alcoholic beverages when drinking (none, 1–2, 3–4, 5–6, 7–9, 10 or more beverages), and how often more than 6 alcoholic beverages are consumed (never, monthly or less, monthly, weekly, daily or almost daily).

Neuropsychological assessment. The neuropsychological examination consisted of a variety of tests measuring global cognitive functioning, verbal intelligence, memory functions, executive functions, and processing speed.

The Montreal Cognitive Assessment (MoCA) was used as a measure of global cognitive functioning [43]. The MoCA consists of 11 items, tapping into several distinct cognitive domains. Visuospatial functions are measured using a cube- and clock-drawing task (4 points). Short-term memory involves learning 5 nouns and delayed recall after an interval of 5 minutes (5 points). Executive functions are measured using an alternation task (1 point), a phonemic fluency task (1 point), and a verbal abstraction task (2 points); attention, concentration and working memory by using a forward and backward digit-span task (2 points), a sustained attention task (1 point), and a serial subtraction task (3 points). Language was assessed using a three-item naming task with animals (3 points), the repetition of two sentences (2 points), and the beforementioned phonemic fluency task. Lastly, orientation to place and time is evaluated using different questions (e.g., "Tell me today's date"; 6 points). As such, a total of 30 points can be obtained.

We used the Dutch Version of the National Adult Reading Test (DART) to obtain a measure of verbal IQ [44]. This test consists of a list of 50 written words that need to be read aloud by the participant that are scored by the experimenter based on pronunciation. To obtain a measure of verbal IQ, the raw scores are corrected for effects of age and sex, and subsequently transformed to indicate verbal IQ, based on Dutch norms. This test is often used as a proxy measure of CR and may be a more sensitive measure of CR than education level [45, 46].

We evaluated memory functions using three different tests: The Story Recall subtest from the Rivermead Behavioural Memory Test–Third Edition (RBMT-3) [47], the Doors Test [48], and the Verbal Paired Associates (VPA) subtest of the Wechsler Memory Scale–Fourth Edition (WMS-IV-NL) [49]. Notably, the VPA was introduced after data was collected for ±100 participants already.

The RBMT-3 evaluates everyday memory functioning by using stimuli that correspond more to everyday life contexts compared to more traditional, laboratory tests of memory. During the Story Recall Subtest, the experimenter reads a 21-element story to the participant with the instructions to repeat as many items as possible afterwards (immediate recall). After an interval of about 15 minutes, the participant is again asked to recall as many elements as possible from this story (delayed recall). Completely correct elements are awarded one point, whereas partially correct elements are awarded half a point.

The Doors Test (part A and B) evaluates visual recognition memory [48]. For each part, participants are presented with 12 different target doors, each presented for 3 seconds. Immediately afterwards, the participant is asked to identify the target door on an array of 2 x 2 doors that includes 3 distractor doors. In part A, the distractors consist of different door types (e.g., a front door vs. a stable door, garage door, and café door). In contrast, distractors of visually similar door types are shown in part B (e.g., all front doors). Each correct response is rewarded with one point, and a total score of 24 can be obtained.

The VPA is a measure of associative memory [49]. The test consists of two parts. First, a list of 14 word-pairs is read to the participant that contains both semantically related (e.g., door-open) and semantically unrelated word pairs (plant-happy). Subsequently, the experimenter provides the participant with the first word of a particular pair and asks the participant to recall the associated word. This procedure is then repeated three times, where the experimenter provides feedback on the participant's responses (immediate recall). Second, after an interval of

20–30 minutes, the participant is asked to recall the paired words, again by providing the participant with the first word of a particular pair, but now without feedback from the experimenter (delayed recall). Subsequently, the delayed recall is followed by a yes/no recognition test of word pairs, and a free-recall test of words from the word pairs. During the free-recall test, the words can be recalled as single items as they do not necessarily have to be recalled within a particular pair. For each part of the VPA, we recorded the participant's responses and the number of correct responses.

We used three different tests to obtain measures for executive functions and processing speed: the Stroop Colour Word Test (SCWT [50]), the Trail Making Test (TMT [51]), and the digit span test (DST) of the Wechsler Memory Scale - Revised (WMS-R) [52].

The SCWT evaluates processing speed and inhibition [50]. Here, participants are asked to perform three tasks as fast as possible: 1) to read names of colours (Word Naming; W); 2) to name different colours (Colour Naming; C); 3) and to name the colour of the ink instead of reading the word itself while the colour-words are displayed in an incongruent colour (Colour-Word Naming; CW). For each task, we recorded the completion time and the number of errors made.

The TMT consists of part A and part B, and allows to measure attention and processing speed [51, 53]. In part A, participants connect a set of 25 consecutive numbers. In part B, a set of 25 circles is connected by alternating between numbers and letters. During both parts, participants are instructed to work as fast and accurately as possible. For each part, the time to complete the task and the number of errors is recorded.

We used the DST to measure working memory [52]. The experimenter reads a list of numbers and asks the participant to recall this list immediately afterwards in forward order. Subsequently, a second list is presented, where the participant is asked to recall the numbers in backward order. For both lists, the total number of digits increases after each sequence of two trials, until the participant fails a complete sequence or reaches the end of the test list that each consists of 6 sequences. The total number of correct reproductions on the forward and the backward versions are recorded.

Cognitive reserve index questionnaire. We used the Cognitive Reserve Index questionnaire (CRIq) to obtain an indication of CR. The CRIq is a semi-structured interview focusing on several proxy measures of CR, namely: education, working activity, and leisure activities. These domains have been suggested to predominantly contribute to the lifetime experiences that contribute to CR [5, 54]. The CRIq hence does not capture CR directly, but instead provides an overall indication of CR that has been accumulated throughout the lifespan as well as sub-scores for each separate domain [54]. Previous literature demonstrated that CRIq scores indeed could explain the discrepancy between cognitive performance and brain pathology in various study populations (i.e., from healthy to pathological ageing), indicating that this is a valid indicator of CR [5, 55].

Self-report questionnaires. Self-report questionnaires included the Beck Depression Inventory, Brief Pain Inventory, Self-Report Psychopathy-short form, and the Metamemory in Adulthood Questionnaire-short form [56–61]. Notably, as mentioned earlier, ongoing efforts to improve the cognitive and behavioural assessment introduced several novel components to the protocol throughout the course of the study. After the inclusion of ±100 participants, the Everyday Memory Questionnaire (revised), Cognitive Failure Questionnaire, and a customized strategy use questionnaire were added to our protocol [62–64].

The Beck Depression Inventory (BDI) was implemented to identify potentially high levels of depressive symptoms and evaluates depressive symptoms on a 4-point scale across 21 items, where higher scores indicate increased presence of depressive symptomatology [56]. A score between 0–9 indicates that an individual is experiencing no or minimal depression, 10–18

indicates mild depression, 19–29 indicates moderate depression, and 30–63 indicates severe depression.

The Brief Pain Inventory (BPI-SF) measures presence and location of pain, pain severity, pain interference on daily functions, pain treatment and (the percentage of) pain relief following treatment. Pain severity (4 items) and pain interference (7 items) are rated on an 11-point rating scale ranging from 0 to 10 [57, 58].

The Self-Report Psychopathy–Short Form (SRP-SF) evaluates psychopathy-related traits [59]. This questionnaire consists of 28 items, rated on a 5-point scale, and comprises four subscales: Interpersonal Manipulation, Callous Affect, Erratic Lifestyle, and Criminal Tendencies.

The Metamemory in Adulthood questionnaire–Short Form (MIA-SF) evaluates subjective memory functions and knowledge of memory processes [60]. In the present study, we use the abridged Dutch version of this questionnaire [61]. The questionnaire consists of 74 items, rated on a 5-point scale, and allows to calculate separate scores for the following domains: Task, Capacity, Change, Anxiety, Achievement, Locus and Strategy. The Strategy domain contains 16 items and is additionally divided into External Strategies (e.g., memory aids, 8 items) and Internal Strategies (e.g., mental imagery, 8 items).

The Everyday Memory Questionnaire–Revised (EMQ) measures subjective memory failure in everyday life [64]. This questionnaire consists of 13 items, rated on a 5-point scale. Each item focuses on the frequency of memory failures in daily life, such as forgetting when a certain event happened (e.g., whether this occurred yesterday or last week), or forgetting to tell someone something important (e.g., passing a message from someone else).

The Cognitive Failure Questionnaire (CFQ) evaluates subjective cognitive functioning and consists of 25 items, rated on a 5-point scale [62, 63]. Each item focuses on the frequency of daily cognitive mistakes, such as missing appointments or experiencing difficulties in making decisions. Four additional questions inform on potential increases in the occurrence of these mistakes and the extent to which an individual finds these experiences troublesome, annoying, or worrisome; however, these items are not used in scoring this questionnaire.

We incorporated a separate, custom-made questionnaire to obtain information on strategy use during the VPA. Here, after completing the VPA, participants are asked to describe whether they used strategies to recall the word pairs, and the type of strategies they used (e.g., concentrating, repetition, visualization, association; see S1 File for an English translation of this questionnaire).

Actigraphy. We used the Actiwatch 2 (Philips Respironics, Eindhoven, the Netherlands), a wristband-type actigraphy device with an internal accelerometer and light sensor to infer sleep-wake rhythms. As we did not have enough devices, we were unable to acquire actigraphy data among all participants. The decision to give a participant an actiwatch was based on the availability of the devices, while also aiming to achieve an equal age distribution of this subsample. Actigraphy was acquired for 7 consecutive days. Participants were asked to report any sleep disorders, as these could affect the data collection (e.g., insomnia, sleep apnea, restless leg syndrome). Epoch length was set at 15 seconds. All data was processed with Actiware software (v6.0.9).

All actograms were visually checked to ensure quality of the data. Data were excluded when the algorithm failed to register any sleep/wake rhythms or was unable to delineate these (e.g., because the device was not worn at all or too irregularly). A minimum of 5 days of usable data was required for inclusion of the data in our database.

With regards to sleep, we recorded the following outcomes measures: total sleep time (summation of sleep epochs within the sleep phases), wake after sleep onset (WASO; summation of wake epochs between begin and end of a sleep phase), sleep latency, sleep efficiency, and number of awakenings. Although this device has been predominantly shown to measure sleep in an

objective and reliable manner [65], recent studies demonstrated that valid measures of physical activity can also be calculated, for example, by using the activity counts per minute or cycle recorded by the device [66].

MRI

Data acquisition. All scans were acquired on a 3T Siemens Magnetom Prisma System (Siemens, Erlangen, Germany) using the standard 32-channel receive coil. We used an auto-align localizer sequence to automatically align all imaging sequences, additionally each alignment was visually checked and manually adjusted when necessary. The duration of the complete scanning session was approximately 55 minutes. Participants were held with head cushions and were additionally fixed using a small piece of tape to reduce head movement [67].

The following MRI scans were acquired: 1) T1-weighted 3D Magnetization Prepared - RApid Gradient Echo (MPRAGE; TR = 2200 ms, TE = 2.64 ms, voxel size 0.8 mm isotropic); 2) T1-weighted MP2RAGE (TR = 6000 ms, TE = 2.34 ms, voxel size 1.0 mm isotropic); 3) Fast turboFLASH B1 mapping (TR = 10000 ms, TE = 2.23 ms, voxel size 3.3x3.3x2.5 mm); 4) T2-weighted turbo spin echo (TSE) sequence (TR = 3200 ms, TE = 569 ms, voxel size = 0.8 mm isotropic); 5) multi-shell High Angular Resolution Diffusion Imaging (HARDI; TR = 2940 ms, TE = 74.80 ms, voxel size 1.8 mm isotropic, 11 x b = 0, 86 x b = 1250, 85 x b = 2500 s/mm2); 6) Multi-echo gradient echo (MEGRE; TR = 44 ms, TE_1 / ΔTE / TE_9 = 6.14 / 4 / 38.14 ms); and 7) 10 minutes resting-state BOLD fMRI (GE-EPI; TR = 1000 ms, TE = 34 ms, voxel size = 2.0 mm isotropic). A complete overview of the sequence parameters can be found in Table 1.

Furthermore, among n = 76 participants, task-based fMRI was collected during a prospective memory paradigm, together with the prospective and retrospective memory questionnaire [68–70]. However, as the prolonged duration of the total MRI scanning protocol (±2.5 hours) led to significant recruitment difficulties, the acquisition of the task was discontinued to preserve the feasibility of the study.

Several efforts were made to facilitate the shareability, reproducibility, and reusability of ABRIM MRI data [71]. First, we adhere to the guidelines outlined in the Brain Imaging Data

Table 1. Overview of neuroimaging sequences and parameters.

Scan type	Sequence	TR (ms)	TE (ms)	Flip angle (˚)	Voxel size (mm)	FOV (RL/AP/FH)	Other
T1-weighted	MPRAGE	2200	2.64	11	0.8x0.8x0.8	180x320x256	GRAPPA: 3; TI = 1100
	MP2RAGE	6000	2.34	6/6	1.0x1.0x1.0	263x350x350	GRAPPA: 3; TI_1/TI_2 = 700/2400
B1 map	turboFLASH	10000	2.23	8	3.3x3.3x2.5	350x263x350	
T2-weighted	TSE	3200	569	n/a	0.8x0.8x0.8	180x320x256	GRAPPA: 3; variable flip angle
Diffusion-weighted	PGSE-EPI	2940	74.80	90	1.8x1.8x1.8	216x216x146	GRAPPA: 2; SMS factor = 3 (interleaved); 11 b = 0 s/mm^2 volumes; 86 b = 1250 s/mm^2; 85 b = 2500 s/mm^2
MEGRE	Bipolar multi-echo GRE	44	TE_1/ΔTE /TE_9 = 6.14/4/38.14	20	0.8x0.8x0.8	186x230x141	GRAPPA: 3
Resting-state fMRI	Multi-band GRE-EPI	1000	34	60	2.0x2.0x2.0	210x210x132	Acquisition time: 10 minutes.
	Inverted Distortion GRE-EPI	1000	34	60	2.0x2.0x2.0	210x210x132	

TR, repetition time; TE, echo time; TI, inversion time; FOV, field of view; MPRAGE, Magnetization Prepared Rapid Acquisition Gradient Echo; GRAPPA, GeneRalized Autocalibrating Partial Parallel Acquisition; MP2RAGE, Magnetization Prepared 2 Rapid Acquisition Gradient Echoes. TSE, Turbo Spin Echo. PGSE, Pulsed-gradient spin-echo. EPI, echo planar imaging. SMS, simultaneous multi-slice. GRE, Gradient Echo Imaging.

https://doi.org/10.1371/journal.pone.0306006.t001

Structure (BIDS) [72], and COBIDAS MRI reporting framework [73]. Second, we used standard containerized neuroimaging pipelines specifically developed for BIDS data (i.e., BIDS apps) [72], to process the raw MRI images and to provide visual quality control (QC) reports. Below, we explain our MRI sequences and (pre-)processing pipelines in more detail. A schematic illustration of the various methodological steps that were applied to each imaging modality, and corresponding BIDS folders, is displayed in Fig 1.

BIDS conversion. To transform raw DICOM files to BIDS, we used version 3.7.4 of the open-source BIDScoin application (https://github.com/Donders-Institute/bidscoin) [76]. The resulting data complied to version 1.8 of the BIDS standard, which was verified by application of the bids-validator version 1.11 (https://github.com/bids-standard/bids-validator) After BIDS conversion was completed for all participants, we proceeded with de-identification of all anatomical MRI data by applying the deface BIDS app of BIDScoin. The deface app is a wrapper of *pydeface* (https://github.com/poldracklab/pydeface) and ensures that the output corresponds to the BIDS standard. All output was visually inspected by one author (MGJ) to ensure successful de-identification, while a second author was consulted (MPZ) in case of any uncertainties. Manual masks were created in case of any remaining unique personal features that could led to potential identification (e.g., nasal features), and masked out from the anatomical images using *fslmaths* from FMRIB Software Library (FSL; https://fsl.fmrib.ox.ac.uk/).

T1- and T2-weighted imaging derivatives. We incorporated the T1-weighted MPRAGE and T2-weighted TSE sequences to allow for the characterization of conventional markers of brain ageing, such as the volume and thickness of various brain regions [77, 78]. Furthermore, these sequences can be combined to obtain more detailed measurements of brain morphology and maps of the structural organization of the cerebral cortex (e.g., relative myelin content) [79]. As explained below, the T1-weighted images are minimally processed together with the resting-state fMRI and diffusion-weighted sequences. For both T1- and T2-weighted images, we provide visual QC reports.

We used the general purpose slicereport-tool of BIDScoin to generate visual QC reports unless otherwise specified. Slicereport facilitates the generation of a web page, displaying rows of image slices for each subject, and optionally provides individual sub-pages with more detailed information. In addition, it provides the flexibility to customize the displayed information. Therefore, slicereport enables efficient and thorough visual inspections of MRI data. For an example of its application in ABRIM, see Fig 2.

Asides from this, we applied the MRI Quality Control tool (MRIQC) to provide additional QC reports and image quality metrics for the T1, T2, and fMRI images [80].

MP2RAGE and Fast turboFLASH B1 mapping. The MP2RAGE sequence was developed to obtain T1-weighted images that are less dependent of transmit and receive field inhomogeneities (B_1^+ and B_1^-) and improve the contrast between white matter and grey matter tissue [39] by removing residual dependency on water density and transverse relaxation (M_0 and T_2^*). We acquired MP2RAGE from which quantitative longitudinal relaxation rate (R_1) and proton density maps were derived [35]. The turbo flash B1 maps were utilized to correct transmit field inhomogeneities. Previous studies revealed that R1 maps are useful to delineate cortical myelination in group studies [37], and to study white matter tissue maturation over the lifespan [81]. Proton density maps can be used to compute the surrogate Macromolecular Tissue Volume fraction [82].

To process the MP2RAGE images, we used BIDS compatible Matlab scripts that are hosted on Github (https://github.com/Donders-Institute/MP2RAGE-related-scripts). For the purpose of anatomical referencing, the typical salt and pepper noise of the MP2RAGE was reduced using the regularization method as described in [83]. Quantitative R1 maps were obtained using bids_T1B1correct.m from the above repository: (i) The magnitude image from the turbo

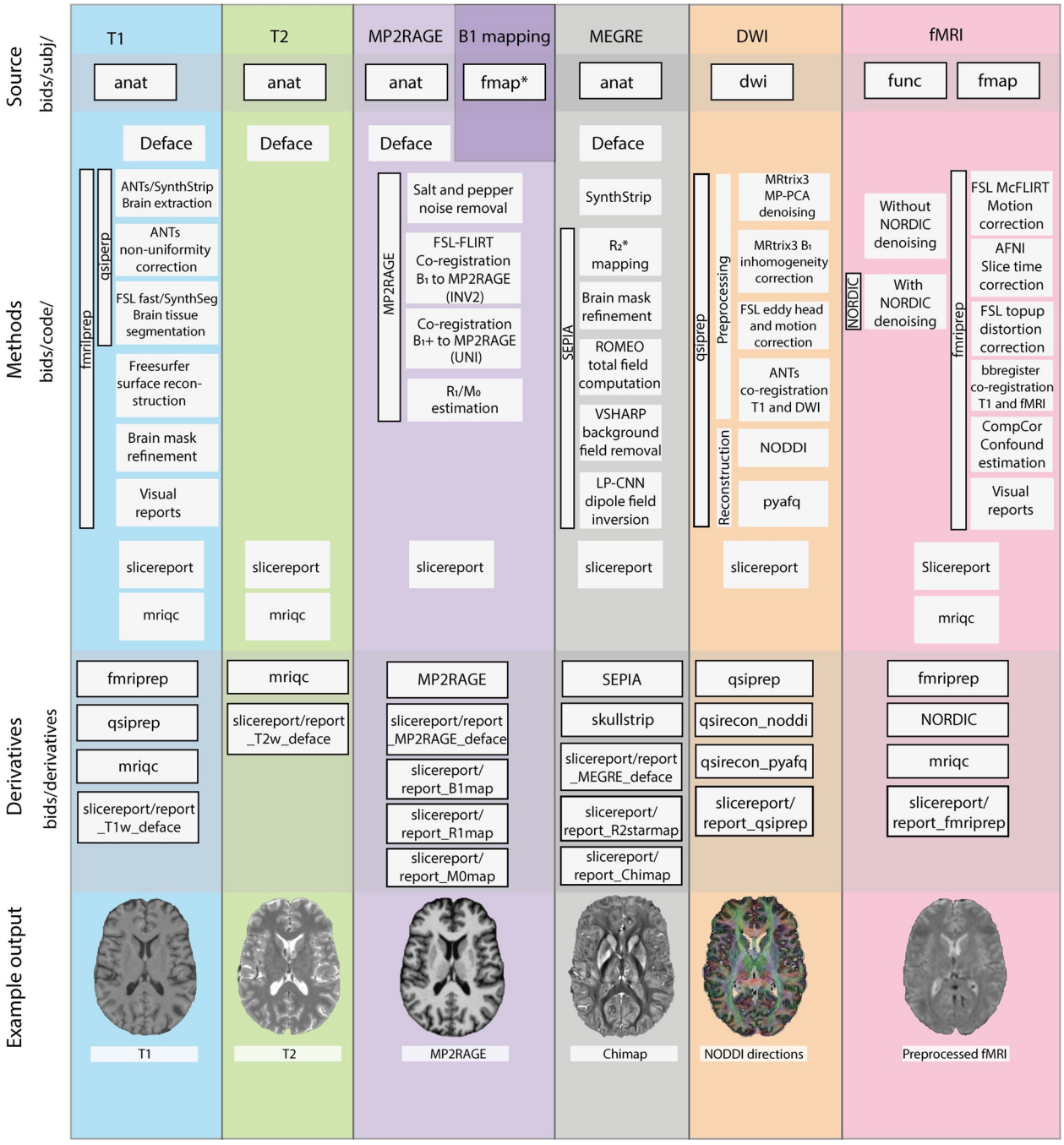

Fig 1. Methodological steps applied to each imaging modality in ABRIM. Schematic illustration of the methodological steps that were applied for each imaging modality, and its corresponding Brain Imaging Data Structure (BIDS) folders of the ABRIM MRI collection. Each column in the figure represents a different imaging modality, and is distinguished by a unique colour (e.g., T1 images in blue). Each row represents a specific methodological step (e.g., fMRIprep [74]) with its corresponding sub-steps (e.g., brain extraction). BIDS folders are denoted with black frames. The process starts with the source data (e.g., bids/subj/anat/ folder) and progresses to the derivatives (e.g., bids/derivatives/fmriprep/ folder). For each imaging modality, an example output image is displayed at the bottom. All code utilized can be found in the bids/code folder. Note that a certain imaging modality may be processed by multiple methods (e.g., T1 images with both fMRIprep and QSIprep [74, 75]). *fmap is available under bids/subj/derivatives/SIEMENS/.

https://doi.org/10.1371/journal.pone.0306006.g001

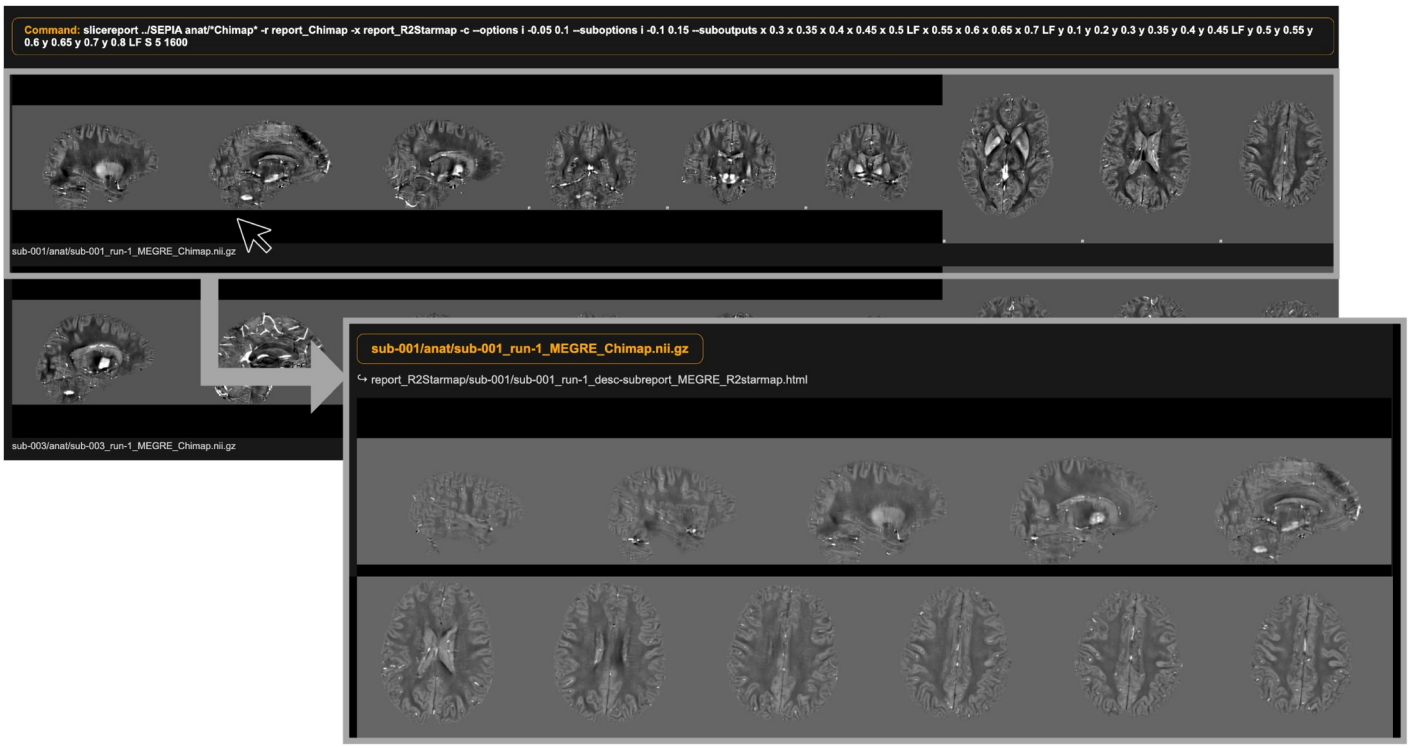

Fig 2. Example of slicereport output for ABRIM. An example of the slicereport-tool to create visual quality control reports for Quantitative Susceptibility Mapping (QSM) output in ABRIM. The top left image displays the generated web page, featuring rows of image slices per subject. In this case, the researchers opted for several sagittal, coronal, and axial slices to enable visual inspection of physiological noise (e.g., motion, ringing) and streaking artifacts. Upon clicking on the image slices of a specific subject, it leads to a sub-page (right bottom image). In this case, the sub-page displays a more detailed representation of the various slice orientations to further facilitate visual inspection. To facilitate the delineation of motion artifact, the sub-page additionally contains a weblink that enables the user to view the corresponding R2* maps ("report_R2Starmap/sub-001/sub-001_run-1_desc-subreport_MEGRE_R2starmap.html").

https://doi.org/10.1371/journal.pone.0306006.g002

flash B1 map was registered to the MP2RAGE image with proton density contrast (INV2) using SPM12 [84]; (ii) The resulting transform matrix was then used to co-register a spatially smoothed version of the B1+ map to the MP2RAGE image; (iii) To correct for B1 transmit inhomogeneities in R1 estimations (and derive M0 maps over a large range of R1 values), instead of the traditional MP2RAGE lookup table, a fingerprinting-like approach was used to estimate R1 [85]. Here, the maximum of the inner product of the signal at the two inversion times is used by a dictionary to determine the voxel R1 and M0. MP2RAGE signal dictionaries were computed at steps 0.005 nominal B1 field. Finally, visual QC reports were generated for the R1 and M0 maps.

Gradient echo imaging. We used MEGRE for apparent transverse relaxation rate (R_2*) mapping and quantitative susceptibility mapping (QSM) to obtain quantitative measurements that relate to local concentrations of iron and myelin in the brain. Both techniques are sensitive to the change of tissue magnetic susceptibility *(χ)*. Conventionally, the magnitude of the MEGRE data is used to derive R2* maps and the phase of the MEGRE data is used for QSM. Previous studies demonstrated that increases of iron and myelin concentration enhance the R2* values [40, 86, 87]. In QSM, however, these two constituents produce opposite image contrasts since iron is paramagnetic (+χ) and myelin is diamagnetic (-χ) with respect to water [40, 86, 88]. As ageing is characterized by changes in both myelination and iron depositions throughout the brain [36, 89], processing both the QSM and R2* maps provides a more

complete picture of these alterations at no extra cost as both maps can be derived from the same data.

We used custom BIDS wrapper code around the SEPIA toolbox (v1.2.2.3) for generation of the R2* and QSM maps [90]. Prior to applying the SEPIA toolbox, we acquired brain masks using SynthStrip, a novel learning-based brain extraction tool with highly accurate performance across different imaging modalities and populations [91]. More specifically, we implemented SynthStrip using the skullstrip BIDS app from BIDScoin.

R2* maps were derived by extracting the magnitude of the MEGRE data based on a closed-form solution [90, 92]. Additionally, we generated the corresponding visual QC reports.

We acquired QSM maps through multiple steps in SEPIA [90]. First, the MEGRE brain masks were initially refined by masking out high R2* voxels on the mask edge associated with non-tissue of interest (e.g., air and vein) that can create strong susceptibility artefacts. Subsequently, total field computation was performed with ROMEO [93], background field removal with VSHARP [94], and dipole field inversion using LP-CNN [95]. As QSM only provides relative values, we used the mean susceptibility of the whole brain as a reference to facilitate data comparison between subjects. Visual QC reports were generated for the QSM maps.

In addition to the QC reports, we provide subjective quality assessment ratings for physiological noise (e.g., motion, ringing) and streaking artifacts in QSM. Both aspects can have a profound impact on the contrast of the resulting images and validity of results [96]. The presence of both quality aspects was visually rated on a scale from 0 (optimal quality) to 5 (multiple / gross artefacts). Subsequently, these scores are summed to indicate the total quality. The quality assessment file also includes a dichotomous rating to indicate if any parts of the cerebellum or cerebrum were missing (0 = complete; 1 = missing).

Diffusion-weighted imaging. Diffusion-weighted imaging allows to investigate the microstructural properties of the brain in a non-invasive manner. We used multi-shell HARDI with 182 diffusion directions (HARDI, 11 x b = 0, 86 x b = 1250, 85 x b = 2500 s/mm^2) to derive different microstructural properties, such as fractional anisotropy (FA) and mean diffusivity (MD) from diffusion tensor imaging (DTI) [97], or neurite density index (NDI) and orientation dispersion index (OD) from neurite orientation dispersion and density imaging (NODDI) [98]. HARDI also allows for fibre tractography, where diffusion-derived measures are modelled along the trajectories of white matter pathways [99]. Age-related differences and neurodegenerative diseases have been frequently related to these metrics, where loss of white matter integrity is typically characterized by decreased FA and increase MD values [100, 101].

It is well-known that diffusion imaging data are sensitive to corruption from various sources of physiological and scanner noise, and that the images are typically geometrically distorted due to local (susceptibility-induced) and global (eddy-current-induced) magnetic field distortions [102]. We used the state-of-the-art BIDS compatible QSIPrep pre-processing pipeline (v0.18.0) to correct for artifacts and to offer high-quality data [75].

In short, QSIprep processes both structural MRI and diffusion MRI, and automatically incorporates pre-configured workflows based on the data provided to estimate various popular HARDI models, QC metrics, and visual QC reports [75]. For ABRIM structural MRI, QSIprep uses Advanced Normalization Tools (ANTs, https://www.nitrc.org/projects/ants) to correct for intensity non-uniformity [103] and for non-linear registration of T1 images to the MNI152 template [104]. Brain extraction is performed using SynthStrip [91], and tissue segmentation using SynthSeg [105]. For ABRIM diffusion data, QSIprep applies MP-PCA denoising as implemented in MRtrix3's dwidenoise (https://www.mrtrix.org/) [106, 107], B1 field inhomogeneity correction using dwibiascorrect from MRtrix3 with the N4 algorithm [103], head motion and eddy current correction using FSL's eddy [108], and rigid co-registration to the T1-weighted image using antsRegistration (ANTs) [104]. The complete QSIprep pre-

processing configuration is described within the ABRIM MRI collection (*/bids/derivatives/qsiprep/logs*).

We subsequently used QSIprep to apply two preconfigured reconstruction workflows. The first workflow (*mrtrix_multishell_msmt_pyafq_tractometry*) distinguishes major white matter pathways and estimates its corresponding tissue properties. More specifically, besides providing FA and MD estimates, this workflow applies automatic fiber-tract quantification (AFQ [109]) [110] and uses IFOD2 from MRtrix3 to generate many more microstructural measures and tractography data [111]. The second workflow (*amico_noddi*) was utilized to estimate the NODDI model [98] with the AMICO implementation [112]. The resulting outputs include the intra-cellular volume fraction (ICVF), isotropic volume fraction (ISOVF), and orientation dispersion (OD).

Resting-state fMRI. Resting-state fMRI was incorporated because of its relation to task-activation, brain network organization and cognition [113, 114]. With advancing age, brain networks are characterized by less distinct functional networks and decreased local efficiency, predominantly among the brain networks responsible for higher order cognitive processes [14].

We applied the BIDS compatible fMRIprep pre-processing pipeline (v23.1.2), which facilitates the pre-processing of structural and fMRI data by combining different software packages [74]. Briefly, T1 images are corrected for intensity non-uniformity and brain extracted using ANTs [103]. Brain surfaces are reconstructed using Freesurfer (v7.3.2. https://surfer.nmr.mgh.harvard.edu/) and used to refine the initially estimated brain mask. Non-linear registration of T1 images to the ICBM152 template is performed with ANTs [104], and brain tissue segmentation with FSL FAST [115]. With regards to fMRI, susceptibility-induced distortion corrections are performed using FSL topup [116], slice time corrections with Analysis of Functional NeuroImages (AFNI, https://afni.nimh.nih.gov/), and motion corrections with FSL McFLIRT [117]. Co-registration between the T1 images and fMRI data is facilitated using bbregister from Freesurfer [84]. Confounds are estimated for nuisance regression using CompCor [118]. In addition, visual QC reports are saved that allow for a complete evaluation of the fMRIprep procedures. The complete fMRIprep pre-processing configuration is described within the ABRIM MRI collection (*bids/derivatives/fmriprep/logs*).

In addition, we applied Noise Reduction with Distribution Corrected (NORDIC) denoising on the fMRI data, using both the magnitude and phase time series (https://github.com/SteenMoeller/NORDIC_Raw), before running the fMRIprep pre-processing pipeline on the denoised data. Briefly, NORDIC allows to further improve the spatial temporal resolution of fMRI data by reducing thermal noise (i.e., white noise due to thermal fluctuations of the subject and/or receive coil). In contrast to more traditional denoising algorithms (e.g., ICA-AROMA [119]), NORDIC does not affect structured, non-white noise (e.g., due to respiration or the cardiac cycle), and therefore complements other algorithms [120, 121].

Results

Sample characteristics

Among the 301 participants tested, 6 participants were excluded from the dataset, either due to incidental MRI findings (*n* = 5*)* or because of the presence of a condition with a profound impact on the brain and cognitive health (*n = 1)*, resulting in 295 participants in the final study sample (53.20% females, median age 52 years, interquartile range [IQR] 36–66). An overview of the demographics of the ABRIM study per age decade is displayed in Fig 3. A more extensive description is provided in S2 Table. Study characteristics of the sub-sample of 108 participants who solely took part in the behavioural and cognitive assessment are provided in S3 Table.

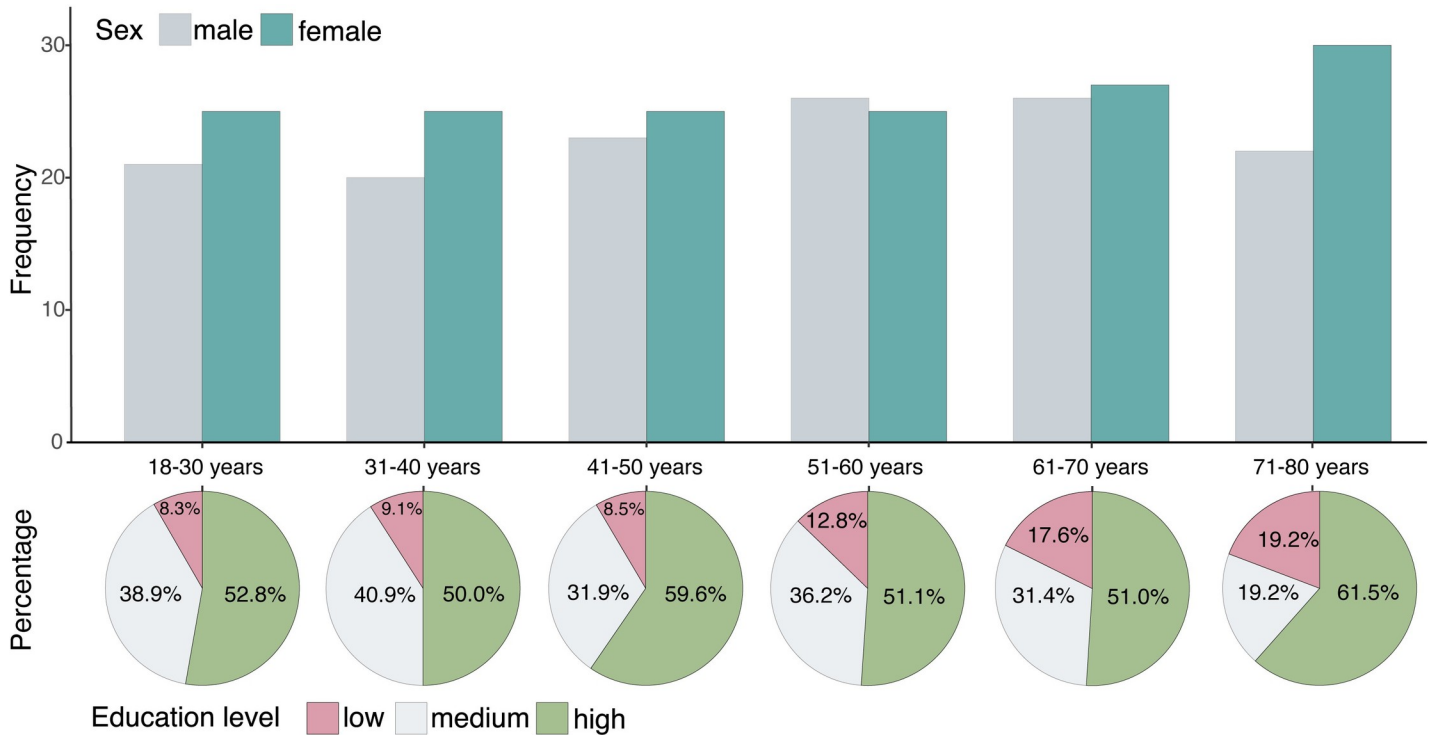

Fig 3. Demographics of the ABRIM study by age decade. The upper section displays the distribution of male and female participants for each age decade. The lower section consists of several pie charts, displaying the relative distribution of participants with low, medium, and high educational attainment within each age decade. Levels of education were classified using the International Classification of Education (ISCED-11): low education (ISCED 0–2), medium education (ISCED 3–4), and high education (ISCED 5–8). Data on educational attainment were not available for $n = 18$ participants.

https://doi.org/10.1371/journal.pone.0306006.g003

Actigraphy data was acquired in a sub-sample of 134 participants. After visually inspecting the data, this resulted in the exclusion of 14 participants ($n = 6$ failed to register any activity, $n = 3$ unable to properly distinguish sleep/wake rhythm, $n = 5$ with less than 5 days of usable data). Therefore, a total of 120 participants were included in our database. Demographics of this sub-sample are displayed in S4 Table. Amongst the sub-sample of participants who only participated in the cognitive and behavioural measurements, actigraphy was acquired among 11 participants ($n = 1$ failed to register any activity and was excluded, resulting in $n = 10$ participants).

ABRIM MRI collection

The ABRIM MRI collection consists of the raw and pre-processed MRI data of 295 participants, together with several automated and/or manual quality control indices in BIDS format. Furthermore, various demographic details are included (age, sex, height, and weight). This collection has been made available on the Radboud Data Repository in December 2023 (https://doi.org/10.34973/7q0a-vj19). Access to the data is available for registered users under the data user agreement for identifiable human data–scientific use (RU-HD-SU-1.0). Detailed instructions are provided on the Radboud Data Repository (https://data.ru.nl/).

A complete overview of the ABRIM BIDS folder structure is provided in Fig 4. Briefly, raw MR images are stored in the subject-specific folders within the bids root directory. These folders additionally contain metadata files that provide a more detailed account of the MRI acquisition parameters. Pre-processed MR images are available in the *bids/derivatives* folder, while the scripts to generate these derivatives are in the *bids/code* folder. Furthermore, within the

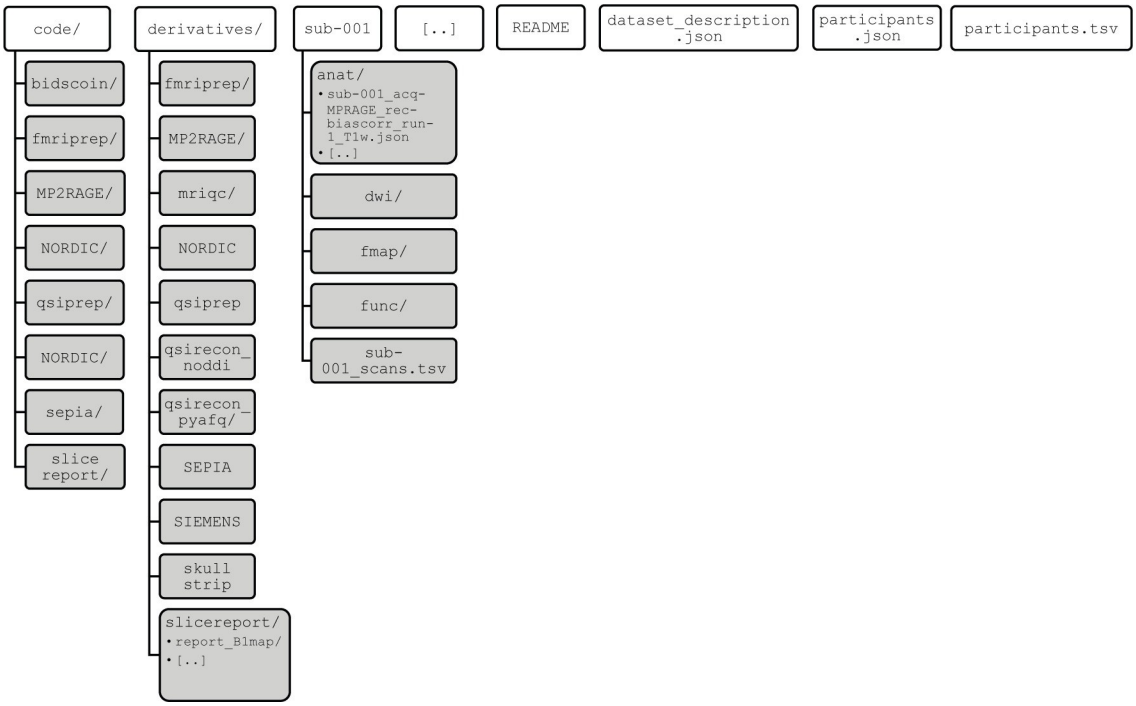

Fig 4. Overview of ABRIM BIDS folder structure. Hierarchical overview of ABRIM MRI data collection folder structure following the Brain Imaging Data Structure (BIDS) standard. The "code" folder contains all scripts that have been applied for data processing. The "derivatives" folder contains all processed and derived data that has been generated from the raw MRI data (e.g., "NORDIC", "SEPIA", etc.). Individual subject-specific folders (e.g., "sub-001", "sub-002", etc.) contain modality-specific sub-folders with different types of MRI data (e.g., "anat" contains structural MRI data, whereas "dwi" contains diffusion-weighted imaging data).

https://doi.org/10.1371/journal.pone.0306006.g004

bids/derivatives folder, we included visual QC reports generated with the slicereport-tool. Examples of the acquired MRI images and derivatives for the ABRIM MRI collection for a single subject are provided in an interactive format in S2 File, covering the sagittal, coronal, and axial orientations.

In addition, we processed the T1-weighted MPRAGE, T2-weighted TSE and resting-state fMRI scans with MRIqc to provide additional QC metrics and group reports. An illustration of the QC group report from MRIqc, derived from the T1-weighted MPRAGE scans, is provided in Fig 5. The QC group reports for the T2-weighted scans and resting-state fMRI images are available in S1 and S2 Figs. For the QSM output, additional subjective quality assessment ratings for physiological noise (e.g., motion, ringing) and streaking artifacts are available in *bids/derivatives/slicereport/report_Chimap/qcscores.tsv*.

ABRIM behavioural collection

This data collection will include the measures obtained from the neuropsychological examination, self-reported questionnaires, and actigraphy. Participants who solely participated in the cognitive and behavioural part prior to the start of the MRI phase are also included, resulting in a total of $n = 404$ participants. Cognitive and behavioural data will be released in November 2028 (ABRIM behavioural collection, https://doi.org/10.34973/7eq5-8y44).

Discussion

To increase our understanding of why we all age differently, an extensive characterization of brain health in concurrence with other factors of risk and resilience in cognitive ageing is

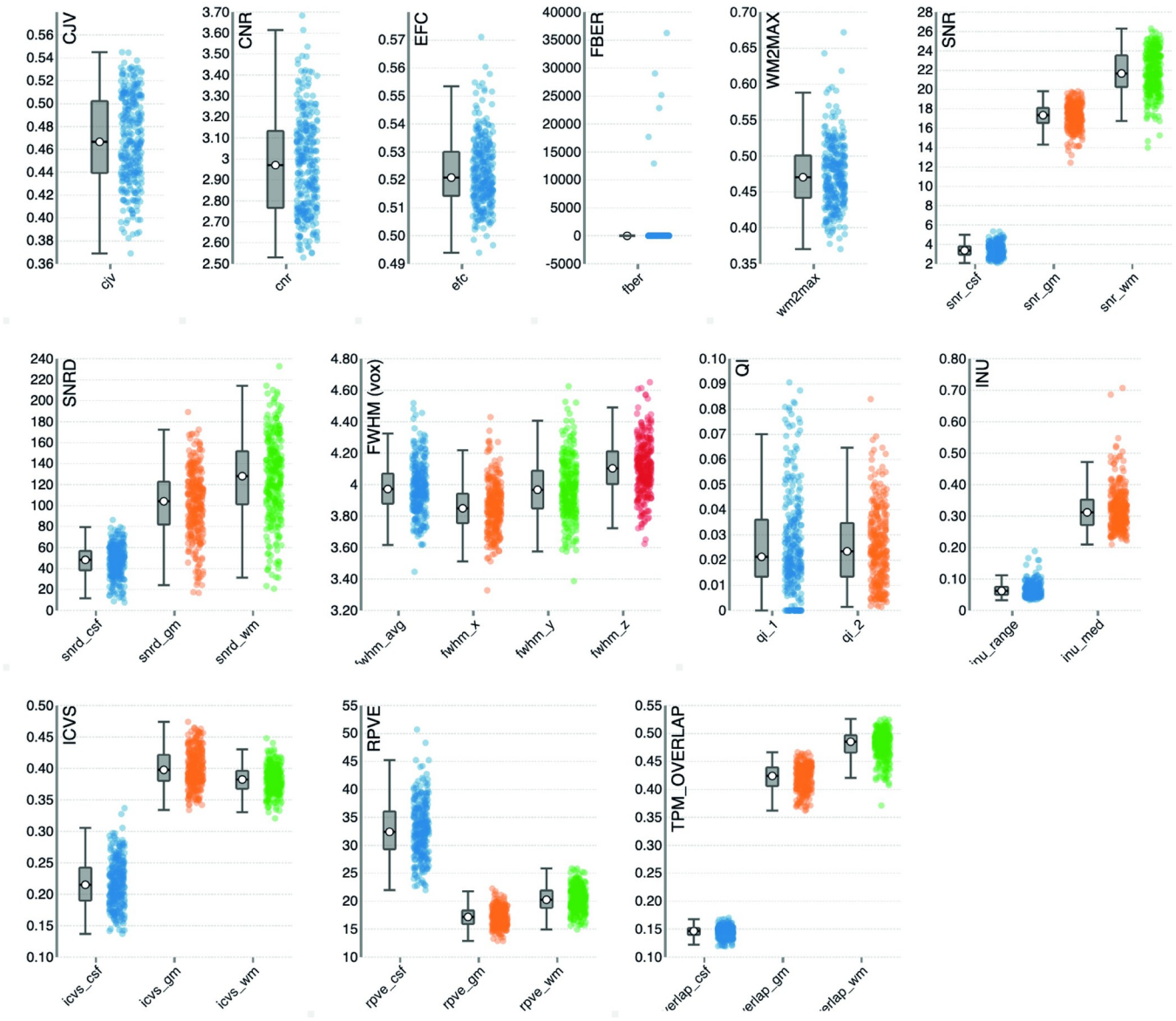

Fig 5. Group report of T1 images from the MRI Quality Control tool. Group anatomical report of T1 scans in ABRIM as generated by the MRI Quality control tool (MRIQC). Contains separate strip-plots for different image quality metrics (IQMs). CJV, coefficient of joint variation; CNR, contrast-to-noise-ratio; EFC, entropy focus criterion; FBER, foreground-to-background energy ratio; WM2MAX white-matter to maximum intensity ratio; SNR, signal-to-noise-ratio; SNRD, Dietrich's signal-to-noise-ratio; FWHM (vox), full width half maximum in units of voxels; QI, quality index; INU, intensity non-uniformity; ICVS, intracranial volume fraction; RPVE, residual partial volume effect; TPM_OVERLAP, overlap of issue probability maps of the images and maps from the ICBM nonlinear-asymmetric 2009a template.

https://doi.org/10.1371/journal.pone.0306006.g005

warranted [2, 6, 17, 20]. Conversely, this has led to the growing availability of large datasets to study the dynamics of cognitive ageing [26–34].

With ABRIM, we aimed to add to existing study cohorts by 1) collecting a cross-sectional, normative database of adults between 18–80 years old, stratified by age and sex; 2) incorporating both conventional imaging sequences as well as quantitative imaging methods; 3) concurrently measuring cognitive functions with mechanisms of reserve (e.g., cognitive reserve), and actigraphy (e.g., to establish sleep-wake rhythms). The present study provides a publicly shared

cross-sectional data repository on healthy adults throughout the lifespan, including numerous parameters relevant to improve our understanding of cognitive ageing.

The ABRIM MRI collection includes BIDS-compliant raw and pre-processed MRI measures and derivatives of T1- and T2-weighted imaging, quantitative imaging (MP2RAGE and gradient echo imaging), multi-shell diffusion-weighted imaging, and resting-state fMRI. The pipelines that we used were specifically developed for BIDS data, facilitating the reproducibility of these analyses [72]. Together with the wide range of MRI measures that are readily available, we hope that this enables both expert and non-expert users to utilize our dataset. To allow users to evaluate the quality of both the raw MR images and pre-processed MR images, we generated several visual QC reports as well as several automated and/or manual quality indices. Importantly, while we emphasize that QC is essential for neuroimaging studies, we refrained from making any decisions about including or excluding specific images modalities or subjects. This decision was made based on the current absence of a "gold-standard" to ensure sufficient quality of MRI data, and because such evaluations may depend on specific research objectives [122]. The ABRIM behavioural data collection complements the MRI measures with the outcomes of a neuropsychological examination (e.g., on executive functioning, processing speed, memory, and global cognition), self-reported questionnaires (e.g., on lifestyle factors, depression, pain, psychopathy, memory strategy use), and actigraphy measures (e.g., sleep-wake parameters).

Nevertheless, there are several limitations that need to be addressed. First, the generalizability of our sample is limited as participants are relatively healthier and more highly educated as compared to the general population. Furthermore, we only covered the adult lifespan between 18–80 years old to minimize potential confounding factors associated with extreme age ranges and for feasibility purposes. Consequently, our sample is not fully reflective of the ageing population. In addition, as ABRIM is a cross-sectional database, this merely allows us to examine cognitive performance within a specific age range at a single point in time, while mapping of individual trajectories of cognitive decline is impossible. Lastly, our sample size remains relatively small as compared to other publicly available datasets. Therefore, we emphasize the importance of replicating findings across multiple cohort studies to increase our understanding of the generalizability and robustness of such data. For instance, comparing MRI measures from ABRIM with those of other currently available datasets itself could provide valuable insights into the consistency of such findings across diverse populations and contexts. We hope that the ABRIM dataset thus will also contribute to open and reproducible research in the field of cognitive ageing and embrace the ongoing growth in availability of such datasets [71].

Conclusion

Altogether, ABRIM enables researchers to model the advanced imaging parameters and cognitive topologies as a function of age, identify the normal range of values of such parameters, and to further investigate the diverse mechanisms of reserve and resilience.

Supporting information

S1 Fig. Group report of T2 images from the MRI Quality Control tool. Group anatomical report of T2 scans in ABRIM as generated by the MRI Quality control tool (MRIQC). Contains separate strip-plots for different image quality metrics (IQMs). CJV, coefficient of joint variation; CNR, contrast-to-noise-ratio; EFC, entropy focus criterion; FBER, foreground-to-background energy ratio; WM2MAX, white-matter to maximum intensity ratio; SNR, signal-to-noise-ratio; SNRD, Dietrich's signal-to-noise-ratio; FWHM (vox), full width half maximum in units of voxels; QI, quality index; INU, intensity non-uniformity; ICVS, intracranial volume

fraction; RPVE, residual partial volume effect; TPM_OVERLAP, overlap of issue probability maps of the images and maps from the ICBM nonlinear-asymmetric 2009a template.
(TIF)

S2 Fig. Group report of fMRI images from the MRI Quality Control tool. Group anatomical report of T2 scans in ABRIM as generated by the MRI Quality control tool (MRIQC). Contains separate strip-plots for different image quality metrics (IQMs). EFC, entropy focus criterion; FBER, foreground-to-background energy ratio; FWHM, full width half maximum in units of millimetres; GSR, ghost-to-signal ratio; SNR, signal-to-noise ratio; DVARS, index of rate of change of BOLD signal across the entire brain; FD, framewise displacement (number of time-points and percentage of timepoints above threshold); DUMMY, number of dummy scans; GCOR, global time-series correlation; TSNR, temporal signal-to-noise ratio; AOR, AFNI's outlier ratio; AQI, AFNI's quality index.
(TIF)

S1 Table. Overview variables in ABRIM relative to other databases.
(PDF)

S2 Table. Sample characteristics of full sample, per age decade and sex. Data on educational attainment were not available for n = 18 participants (6.4% of the total sample). For females and males, the respective numbers were n = 11 (7% of all females) and n = 7 (5.1% of all males).
(PDF)

S3 Table. Sample characteristics of behavioural and cognitive assessment only participants. Data on educational attainment was not available for n = 3 participants (2.8%).
(PDF)

S4 Table. Characteristics of actigraphy sample. Data on educational attainment was not available for n = 5 participants (4.2%).
(PDF)

S1 File. English translation of memory strategy description.
(PDF)

S2 File. Examples of acquired MRI images and derivatives in the ABRIM MRI collection.
(HTML)

Acknowledgments

We express our gratitude to all ABRIM participants for their valuable contributions and dedication of their time.

Author Contributions

Conceptualization: Marcel P. Zwiers, Jose P. Marques.

Data curation: Michelle G. Jansen, Marcel P. Zwiers, Jose P. Marques, Kwok-Shing Chan.

Formal analysis: Michelle G. Jansen, Marcel P. Zwiers, Jose P. Marques, Kwok-Shing Chan.

Funding acquisition: Joukje M. Oosterman, David G. Norris.

Investigation: Michelle G. Jansen, Joukje M. Oosterman.

Methodology: Michelle G. Jansen, Marcel P. Zwiers, Jose P. Marques, Kwok-Shing Chan, Jitse S. Amelink, Mareike Altgassen, Joukje M. Oosterman, David G. Norris.

Project administration: Michelle G. Jansen, Joukje M. Oosterman, David G. Norris.

Resources: Mareike Altgassen, Joukje M. Oosterman, David G. Norris.

Software: Marcel P. Zwiers, Jose P. Marques, Kwok-Shing Chan.

Supervision: Jose P. Marques, Joukje M. Oosterman, David G. Norris.

Visualization: Michelle G. Jansen, Marcel P. Zwiers.

Writing – original draft: Michelle G. Jansen.

Writing – review & editing: Michelle G. Jansen, Marcel P. Zwiers, Jose P. Marques, Kwok-Shing Chan, Jitse S. Amelink, Mareike Altgassen, Joukje M. Oosterman, David G. Norris.

References

1. Beard JR, Officer A, de Carvalho IA, Sadana R, Pot AM, Michel JP, et al. The World report on ageing and health: a policy framework for healthy ageing. Lancet. 2016; 387(10033):2145–54 https://doi.org/10.1016/S0140-6736(15)00516-4 PMID: 26520231
2. Livingston G, Huntley J, Sommerlad A, Ames D, Ballard C, Banerjee S, et al. Dementia prevention, intervention, and care: 2020 report of the Lancet Commission. Lancet. 2020; 396(10248):413–46 https://doi.org/10.1016/S0140-6736(20)30367-6 PMID: 32738937
3. Salthouse TA. Trajectories of normal cognitive aging. Psychol Aging. 2019; 34(1):17–24 https://doi.org/10.1037/pag0000288 PMID: 30211596
4. Salthouse TA. Theoretical perspectives on cognitive aging: Psychology Press; 2016.
5. Stern Y, Arenaza-Urquijo EM, Bartres-Faz D, Belleville S, Cantilon M, Chetelat G, et al. Whitepaper: Defining and investigating cognitive reserve, brain reserve, and brain maintenance. Alzheimers Dement. 2020; 16(9):1305–11 https://doi.org/10.1016/j.jalz.2018.07.219 PMID: 30222945
6. Cabeza R, Albert M, Belleville S, Craik FIM, Duarte A, Grady CL, et al. Maintenance, reserve and compensation: the cognitive neuroscience of healthy ageing. Nat Rev Neurosci. 2018; 19(11):701–10 https://doi.org/10.1038/s41583-018-0068-2 PMID: 30305711
7. Cabeza R, Nyberg L, Park DC. Cognitive neuroscience of aging: Linking cognitive and cerebral aging: Oxford University Press; 2016.
8. Fjell AM, Walhovd KB. Structural brain changes in aging: courses, causes and cognitive consequences. Rev Neurosci. 2010; 21(3):187–221 https://doi.org/10.1515/revneuro.2010.21.3.187 PMID: 20879692
9. Fjell AM, Westlye LT, Grydeland H, Amlien I, Espeseth T, Reinvang I, et al. Accelerating cortical thinning: unique to dementia or universal in aging? Cereb Cortex. 2014; 24(4):919–34 https://doi.org/10.1093/cercor/bhs379 PMID: 23236213
10. Bennett IJ, Madden DJ. Disconnected aging: cerebral white matter integrity and age-related differences in cognition. Neuroscience. 2014; 276:187–205 https://doi.org/10.1016/j.neuroscience.2013.11.026 PMID: 24280637
11. Grydeland H, Walhovd KB, Tamnes CK, Westlye LT, Fjell AM. Intracortical myelin links with performance variability across the human lifespan: results from T1- and T2-weighted MRI myelin mapping and diffusion tensor imaging. J Neurosci. 2013; 33(47):18618–30 https://doi.org/10.1523/JNEUROSCI.2811-13.2013 PMID: 24259583
12. Buyanova IS, Arsalidou M. Cerebral white matter myelination and relations to age, gender, and cognition: A selective review. Front Hum Neurosci. 2021; 15:662031 https://doi.org/10.3389/fnhum.2021.662031 PMID: 34295229
13. Howard CM, Jain S, Cook AD, Packard LE, Mullin HA, Chen NK, et al. Cortical iron mediates age-related decline in fluid cognition. Hum Brain Mapp. 2022; 43(3):1047–60 https://doi.org/10.1002/hbm.25706 PMID: 34854172
14. Geerligs L, Renken RJ, Saliasi E, Maurits NM, Lorist MM. A brain-wide study of age-related changes in functional connectivity. Cereb Cortex. 2015; 25(7):1987–99 https://doi.org/10.1093/cercor/bhu012 PMID: 24532319

15. Ferreira LK, Busatto GF. Resting-state functional connectivity in normal brain aging. Neurosci Biobehav Rev. 2013; 37(3):384–400 https://doi.org/10.1016/j.neubiorev.2013.01.017 PMID: 23333262

16. Poulakis K, Reid RI, Przybelski SA, Knopman DS, Graff-Radford J, Lowe VJ, et al. Longitudinal deterioration of white-matter integrity: heterogeneity in the ageing population. Brain Commun. 2021; 3(1): fcaa238 https://doi.org/10.1093/braincomms/fcaa238 PMID: 33615218

17. Nyberg L, Pudas S. Successful memory aging. Annu Rev Psychol. 2019; 70:219–43 https://doi.org/10.1146/annurev-psych-010418-103052 PMID: 29949727

18. Patel R, Mackay CE, Jansen MG, Devenyi GA, O'Donoghue MC, Kivimaki M, et al. Inter- and intra-individual variation in brain structural-cognition relationships in aging. Neuroimage. 2022; 257:119254 https://doi.org/10.1016/j.neuroimage.2022.119254 PMID: 35490915

19. Biondo F, Jewell A, Pritchard M, Aarsland D, Steves CJ, Mueller C, Cole JH. Brain-age is associated with progression to dementia in memory clinic patients. Neuroimage Clin. 2022; 36:103175 https://doi.org/10.1016/j.nicl.2022.103175 PMID: 36087560

20. Baumgart M, Snyder HM, Carrillo MC, Fazio S, Kim H, Johns H. Summary of the evidence on modifiable risk factors for cognitive decline and dementia: A population-based perspective. Alzheimers Dement. 2015; 11(6):718–26 https://doi.org/10.1016/j.jalz.2015.05.016 PMID: 26045020

21. Gardener H, Wright CB, Rundek T, Sacco RL. Brain health and shared risk factors for dementia and stroke. Nat Rev Neurol. 2015; 11(11):651–7 https://doi.org/10.1038/nrneurol.2015.195 PMID: 26481296

22. Han LKM, Schnack HG, Brouwer RM, Veltman DJ, van der Wee NJA, van Tol MJ, et al. Contributing factors to advanced brain aging in depression and anxiety disorders. Transl Psychiatry. 2021; 11 (1):402 https://doi.org/10.1038/s41398-021-01524-2 PMID: 34290222

23. Barulli D, Stern Y. Efficiency, capacity, compensation, maintenance, plasticity: emerging concepts in cognitive reserve. Trends Cogn Sci. 2013; 17(10):502–9 https://doi.org/10.1016/j.tics.2013.08.012 PMID: 24018144

24. Pettigrew C, Soldan A. Defining cognitive reserve and implications for cognitive aging. Curr Neurol Neurosci Rep. 2019; 19(1):1 https://doi.org/10.1007/s11910-019-0917-z PMID: 30627880

25. Boyle PA, Wang T, Yu L, Wilson RS, Dawe R, Arfanakis K, et al. To what degree is late life cognitive decline driven by age-related neuropathologies? Brain. 2021; 144(7):2166–75 https://doi.org/10.1093/brain/awab092 PMID: 33742668

26. Babayan A, Erbey M, Kumral D, Reinelt JD, Reiter AMF, Robbig J, et al. A mind-brain-body dataset of MRI, EEG, cognition, emotion, and peripheral physiology in young and old adults. Sci Data. 2019; 6 (1):180308 https://doi.org/10.1038/sdata.2018.308 PMID: 30747911

27. Spreng RN, Setton R, Alter U, Cassidy BN, Darboh B, DuPre E, et al. Neurocognitive aging data release with behavioral, structural and multi-echo functional MRI measures. Sci Data. 2022; 9(1):119 https://doi.org/10.1038/s41597-022-01231-7 PMID: 35351925

28. Nugent AC, Thomas AG, Mahoney M, Gibbons A, Smith JT, Charles AJ, et al. The NIMH intramural healthy volunteer dataset: A comprehensive MEG, MRI, and behavioral resource. Sci Data. 2022; 9 (1):518 https://doi.org/10.1038/s41597-022-01623-9 PMID: 36008415

29. Bookheimer SY, Salat DH, Terpstra M, Ances BM, Barch DM, Buckner RL, et al. The Lifespan Human Connectome Project in Aging: An overview. Neuroimage. 2019; 185:335–48 https://doi.org/10.1016/j.neuroimage.2018.10.009 PMID: 30332613

30. Filippini N, Zsoldos E, Haapakoski R, Sexton CE, Mahmood A, Allan CL, et al. Study protocol: The Whitehall II imaging sub-study. BMC Psychiatry. 2014; 14(1):159 https://doi.org/10.1186/1471-244X-14-159 PMID: 24885374

31. Taylor JR, Williams N, Cusack R, Auer T, Shafto MA, Dixon M, et al. The Cambridge Centre for Ageing and Neuroscience (Cam-CAN) data repository: Structural and functional MRI, MEG, and cognitive data from a cross-sectional adult lifespan sample. Neuroimage. 2017; 144(Pt B):262–9 https://doi.org/10.1016/j.neuroimage.2015.09.018 PMID: 26375206

32. Wardlaw JM, Bastin ME, Valdes Hernandez MC, Maniega SM, Royle NA, Morris Z, et al. Brain aging, cognition in youth and old age and vascular disease in the Lothian Birth Cohort 1936: rationale, design and methodology of the imaging protocol. Int J Stroke. 2011; 6(6):547–59 https://doi.org/10.1111/j.1747-4949.2011.00683.x PMID: 22111801

33. Miller KL, Alfaro-Almagro F, Bangerter NK, Thomas DL, Yacoub E, Xu J, et al. Multimodal population brain imaging in the UK Biobank prospective epidemiological study. Nat Neurosci. 2016; 19(11):1523–36 https://doi.org/10.1038/nn.4393 PMID: 27643430

34. Taylor AM, Pattie A, Deary IJ. Cohort Profile Update: The Lothian Birth Cohorts of 1921 and 1936. Int J Epidemiol. 2018; 47(4):1042-r https://doi.org/10.1093/ije/dyy022 PMID: 29546429

35. Marques JP, Gruetter R. New developments and applications of the MP2RAGE sequence—focusing the contrast and high spatial resolution R1 mapping. Plos One. 2013; 8(7):e69294 https://doi.org/10.1371/journal.pone.0069294 PMID: 23874936

36. Khattar N, Triebswetter C, Kiely M, Ferrucci L, Resnick SM, Spencer RG, et al. Investigation of the association between cerebral iron content and myelin content in normative aging using quantitative magnetic resonance neuroimaging. Neuroimage. 2021; 239:118267 https://doi.org/10.1016/j.neuroimage.2021.118267 PMID: 34139358

37. Shams Z, Norris DG, Marques JP. A comparison of in vivo MRI based cortical myelin mapping using T1w/T2w and R1 mapping at 3T. Plos One. 2019; 14(7):e0218089 https://doi.org/10.1371/journal.pone.0218089 PMID: 31269041

38. Ghadery C, Pirpamer L, Hofer E, Langkammer C, Petrovic K, Loitfelder M, et al. R2* mapping for brain iron: associations with cognition in normal aging. Neurobiol Aging. 2015; 36(2):925–32 https://doi.org/10.1016/j.neurobiolaging.2014.09.013 PMID: 25443291

39. Marques JP, Kober T, Krueger G, van der Zwaag W, Van de Moortele P-F, Gruetter R. MP2RAGE, a self bias-field corrected sequence for improved segmentation and T1-mapping at high field. Neuroimage. 2010; 49(2):1271–81 https://doi.org/10.1016/j.neuroimage.2009.10.002 PMID: 19819338

40. Langkammer C, Krebs N, Goessler W, Scheurer E, Ebner F, Yen K, et al. Quantitative MR imaging of brain iron: a postmortem validation study. Radiology. 2010; 257(2):455–62 https://doi.org/10.1148/radiol.10100495 PMID: 20843991

41. Wilkinson MD, Dumontier M, Aalbersberg IJ, Appleton G, Axton M, Baak A, et al. The FAIR Guiding Principles for scientific data management and stewardship. Sci Data. 2016; 3(1):160018 https://doi.org/10.1038/sdata.2016.18 PMID: 26978244

42. UNESCO. International Standard Classification of Education (ISCED). Montreal, Canada: UNESCO-UIS; 2011.

43. Nasreddine ZS, Phillips NA, Bedirian V, Charbonneau S, Whitehead V, Collin I, et al. The Montreal Cognitive Assessment, MoCA: a brief screening tool for mild cognitive impairment. J Am Geriatr Soc. 2005; 53(4):695–9 https://doi.org/10.1111/j.1532-5415.2005.53221.x PMID: 15817019

44. Schmand B, Bakker D, Saan R, Louman J. [The Dutch Reading Test for Adults: a measure of premorbid intelligence level]. Tijdschr Gerontol Geriatr. 1991; 22(1):15–9.

45. Opdebeeck C, Martyr A, Clare L. Cognitive reserve and cognitive function in healthy older people: a meta-analysis. Neuropsychol Dev Cogn B Aging Neuropsychol Cogn. 2016; 23(1):40–60 https://doi.org/10.1080/13825585.2015.1041450 PMID: 25929288

46. Boyle R, Knight SP, De Looze C, Carey D, Scarlett S, Stern Y, et al. Verbal intelligence is a more robust cross-sectional measure of cognitive reserve than level of education in healthy older adults. Alzheimers Res Ther. 2021; 13(1):128 https://doi.org/10.1186/s13195-021-00870-z PMID: 34253231

47. Wilson BA. The Rivermead Behavioural Memory Test - Third Edition: RBMT 3 Administration and scoring manual. London: Pearson; 2008.

48. Baddeley A, Emslie H, Nimmo-Smith I. The Doors and People Test: A test of visual and verbal recall and recognition. Bury-St-Edmunds, United Kingdom: Thames Valley Test. 1994.

49. Hendriks MPH, Bouman Z, Kessels RPC, Aldenkamp AP. Wechsler Memory Scale–Fourth Edition, Dutch Edition (WMS-IV-NL). Amsterdam: Pearson; 2014.

50. Houx PJ, Jolles J, Vreeling FW. Stroop interference: aging effects assessed with the Stroop Color-Word Test. Exp Aging Res. 1993; 19(3):209–24 https://doi.org/10.1080/03610739308253934 PMID: 8223823

51. Reitan RM. Validity of the Trail Making Test as an indicator of organic brain damage. Percept. Mot. Skills. 1958; 8(3):271–6 https://doi.org/10.2466/pms.1958.8.3.271

52. Wechsler D. Wechsler Memory Scale–Revised (WMS-R). San Antonio: The Psychological Corporation: 1987.

53. Reitan RM. The relation of the trail making test to organic brain damage. J Consult Psychol. 1955; 19(5):393–4 https://doi.org/10.1037/h0044509 PMID: 13263471

54. Nucci M, Mapelli D, Mondini S. Cognitive Reserve Index questionnaire (CRIq): a new instrument for measuring cognitive reserve. Aging Clin Exp Res. 2012; 24(3):218–26 https://doi.org/10.3275/7800 PMID: 21691143

55. Kartschmit N, Mikolajczyk R, Schubert T, Lacruz ME. Measuring Cognitive Reserve (CR) - A systematic review of measurement properties of CR questionnaires for the adult population. Plos One. 2019; 14(8):e0219851 https://doi.org/10.1371/journal.pone.0219851 PMID: 31390344

56. Beck AT, Steer RA. Manual for the Beck depression inventory. San Antonio: The psychological corporation 1987.

57. Cleeland CS, Ryan KM. Pain assessment: global use of the Brief Pain Inventory. Ann Acad Med Singap. 1994; 23(2):129–38. PMID: 8080219

58. Tan G, Jensen MP, Thornby JI, Shanti BF. Validation of the Brief Pain Inventory for chronic nonmalignant pain. J Pain. 2004; 5(2):133–7 https://doi.org/10.1016/j.jpain.2003.12.005 PMID: 15042521

59. Paulhus DL, Neumann CS, Hare RD. Manual for the self-report psychopathy scale. Toronto: Multi-health systems; 2009.

60. Dixon RA, Hultsch DF, Hertzog C. The Metamemory in Adulthood (MIA) questionnaire. Psychopharmacol Bull. 1988; 24(4):671–88. PMID: 3249770

61. Ponds RW, Jolles J. The Abridged Dutch Metamemory in Adulthood (MIA) Questionnaire: structure and effects of age, sex, and education. Psychol Aging. 1996; 11(2):324–32 https://doi.org/10.1037//0882-7974.11.2.324 PMID: 8795061

62. Broadbent DE, Cooper PF, FitzGerald P, Parkes KR. The Cognitive Failures Questionnaire (CFQ) and its correlates. Br J Clin Psychol. 1982; 21(1):1–16 https://doi.org/10.1111/j.2044-8260.1982.tb01421.x PMID: 7126941

63. Ponds R, Van Boxtel M, Jolles J. [The Cognitive Failure Questionnaire as a measure of subjective cognitive decline]. Tijdsch. Neuropsych. 2006; 2:37–45.

64. Royle J, Lincoln NB. The Everyday Memory Questionnaire-revised: development of a 13-item scale. Disabil Rehabil. 2008; 30(2):114–21 https://doi.org/10.1080/09638280701223876 PMID: 17852284

65. Shin M, Swan P, Chow CM. The validity of Actiwatch2 and SenseWear armband compared against polysomnography at different ambient temperature conditions. Sleep Sci. 2015; 8(1):9–15 https://doi.org/10.1016/j.slsci.2015.02.003 PMID: 26483937

66. Neil-Sztramko SE, Rafn BS, Gotay CC, Campbell KL. Determining activity count cut-points for measurement of physical activity using the Actiwatch2 accelerometer. Physiol Behav. 2017; 173:95–100 https://doi.org/10.1016/j.physbeh.2017.01.026 PMID: 28108333

67. Krause F, Benjamins C, Eck J, Lührs M, van Hoof R, Goebel R. Active head motion reduction in magnetic resonance imaging using tactile feedback. Hum Brain Mapp. 2019; 40(14):4026–37. https://doi.org/10.1002/hbm.24683 PMID: 31179609

68. Altgassen M, Cohen AL, Jansen MG. The effects of collaboration and punishment on prospective memory performance in a group setting. Appl Cogn Psychol. 2021; 35(1):160–8 https://doi.org/10.1002/acp.3748

69. Altgassen M, Kretschmer A, Schnitzspahn KM. Future thinking instructions improve prospective memory performance in adolescents. Child Neuropsychology. 2017; 23(5):536–53 https://doi.org/10.1080/09297049.2016.1158247 PMID: 27018038

70. Smith G, Del Sala S, Logie RH, Maylor EA. Prospective and retrospective memory in normal ageing and dementia: A questionnaire study. Memory. 2000; 8(5):311–21 https://doi.org/10.1080/09658210050117735 PMID: 11045239

71. Niso G, Botvinik-Nezer R, Appelhoff S, De La Vega A, Esteban O, Etzel JA, et al. Open and reproducible neuroimaging: From study inception to publication. Neuroimage. 2022; 263:119623 https://doi.org/10.1016/j.neuroimage.2022.119623 PMID: 36100172

72. Gorgolewski KJ, Auer T, Calhoun VD, Craddock RC, Das S, Duff EP, et al. The brain imaging data structure, a format for organizing and describing outputs of neuroimaging experiments. Sci Data. 2016; 3(1):160044 https://doi.org/10.1038/sdata.2016.44 PMID: 27326542

73. Nichols TE, Das S, Eickhoff SB, Evans AC, Glatard T, Hanke M, et al. Best practices in data analysis and sharing in neuroimaging using MRI. Nat Neurosci. 2017; 20(3):299–303 https://doi.org/10.1038/nn.4500 PMID: 28230846

74. Esteban O, Markiewicz CJ, Blair RW, Moodie CA, Isik AI, Erramuzpe A, et al. fMRIPrep: a robust preprocessing pipeline for functional MRI. Nat Methods. 2019; 16(1):111–6 https://doi.org/10.1038/s41592-018-0235-4 PMID: 30532080

75. Cieslak M, Cook PA, He X, Yeh FC, Dhollander T, Adebimpe A, et al. QSIPrep: an integrative platform for preprocessing and reconstructing diffusion MRI data. Nat Methods. 2021; 18(7):775–8 https://doi.org/10.1038/s41592-021-01185-5 PMID: 34155395

76. Zwiers MP, Moia S, Oostenveld R. BIDScoin: A user-friendly application to convert source data to Brain Imaging Data Structure. Front Neuroinform. 2021; 15:770608 https://doi.org/10.3389/fninf.2021.770608 PMID: 35095452

77. Rutherford S, Fraza C, Dinga R, Kia SM, Wolfers T, Zabihi M, et al. Charting brain growth and aging at high spatial precision. Elife. 2022; 11:e72904 https://doi.org/10.7554/eLife.72904 PMID: 35101172

78. Bethlehem RAI, Seidlitz J, White SR, Vogel JW, Anderson KM, Adamson C, et al. Brain charts for the human lifespan. Nature. 2022; 604(7906):525–33 https://doi.org/10.1038/s41586-022-04554-y PMID: 35388223

79. Glasser MF, Coalson TS, Robinson EC, Hacker CD, Harwell J, Yacoub E, et al. A multi-modal parcellation of human cerebral cortex. Nature. 2016; 536(7615):171–8 https://doi.org/10.1038/nature18933 PMID: 27437579

80. Esteban O, Birman D, Schaer M, Koyejo OO, Poldrack RA, Gorgolewski KJ. MRIQC: Advancing the automatic prediction of image quality in MRI from unseen sites. Plos One. 2017; 12(9):e0184661 https://doi.org/10.1371/journal.pone.0184661 PMID: 28945803

81. Yeatman JD, Wandell BA, Mezer AA. Lifespan maturation and degeneration of human brain white matter. Nat Commun. 2014; 5(1):4932 https://doi.org/10.1038/ncomms5932 PMID: 25230200

82. Mezer A, Yeatman JD, Stikov N, Kay KN, Cho NJ, Dougherty RF, et al. Quantifying the local tissue volume and composition in individual brains with magnetic resonance imaging. Nat Med. 2013; 19 (12):1667–72 https://doi.org/10.1038/nm.3390 PMID: 24185694

83. O'Brien KR, Kober T, Hagmann P, Maeder P, Marques J, Lazeyras F, et al. Robust T1-weighted structural brain imaging and morphometry at 7T using MP2RAGE. Plos One. 2014; 9(6):e99676 https://doi.org/10.1371/journal.pone.0099676 PMID: 24932514

84. Greve DN, Fischl B. Accurate and robust brain image alignment using boundary-based registration. Neuroimage. 2009; 48(1):63–72 https://doi.org/10.1016/j.neuroimage.2009.06.060 PMID: 19573611

85. Ma D, Gulani V, Seiberlich N, Liu K, Sunshine JL, Duerk JL, et al. Magnetic resonance fingerprinting. Nature. 2013; 495(7440):187–92 https://doi.org/10.1038/nature11971 PMID: 23486058

86. Lee J, Shmueli K, Kang BT, Yao B, Fukunaga M, van Gelderen P, et al. The contribution of myelin to magnetic susceptibility-weighted contrasts in high-field MRI of the brain. Neuroimage. 2012; 59 (4):3967–75 https://doi.org/10.1016/j.neuroimage.2011.10.076 PMID: 22056461

87. Langkammer C, Krebs N, Goessler W, Scheurer E, Yen K, Fazekas F, et al. Susceptibility induced gray-white matter MRI contrast in the human brain. Neuroimage. 2012; 59(2):1413–9 https://doi.org/10.1016/j.neuroimage.2011.08.045 PMID: 21893208

88. Liu C, Li W, Tong KA, Yeom KW, Kuzminski S. Susceptibility-weighted imaging and quantitative susceptibility mapping in the brain. J Magn Reson Imaging. 2015; 42(1):23–41 https://doi.org/10.1002/jmri.24768 PMID: 25270052

89. Betts MJ, Acosta-Cabronero J, Cardenas-Blanco A, Nestor PJ, Duzel E. High-resolution characterisation of the aging brain using simultaneous quantitative susceptibility mapping (QSM) and R2* measurements at 7T. Neuroimage. 2016; 138:43–63 https://doi.org/10.1016/j.neuroimage.2016.05.024 PMID: 27181761

90. Chan KS, Marques JP. SEPIA-Susceptibility mapping pipeline tool for phase images. Neuroimage. 2021; 227:117611 https://doi.org/10.1016/j.neuroimage.2020.117611 PMID: 33309901

91. Hoopes A, Mora JS, Dalca AV, Fischl B, Hoffmann M. SynthStrip: skull-stripping for any brain image. Neuroimage. 2022; 260:119474 https://doi.org/10.1016/j.neuroimage.2022.119474 PMID: 35842095

92. Gil R, Khabipova D, Zwiers M, Hilbert T, Kober T, Marques JP. An in vivo study of the orientation-dependent and independent components of transverse relaxation rates in white matter. NMR Biomed. 2016; 29(12):1780–90 https://doi.org/10.1002/nbm.3616 PMID: 27809376

93. Dymerska B, Eckstein K, Bachrata B, Siow B, Trattnig S, Shmueli K, Robinson SD. Phase unwrapping with a rapid opensource minimum spanning tree algorithm (ROMEO). Magn Reson Med. 2021; 85 (4):2294–308 https://doi.org/10.1002/mrm.28563 PMID: 33104278

94. Li W, Wu B, Liu C. Quantitative susceptibility mapping of human brain reflects spatial variation in tissue composition. Neuroimage. 2011; 55(4):1645–56 https://doi.org/10.1016/j.neuroimage.2010.11.088 PMID: 21224002

95. Lai K-W, Aggarwal M, Pv Zijl, Li X, Sulam J, editors. Learned proximal networks for quantitative susceptibility mapping. International Conference on Medical Image Computing and Computer-Assisted Intervention; 2020: Springer. https://doi.org/10.1007/978-3-030-59713-9_13 PMID: 33163993

96. Marques JP, Meineke J, Milovic C, Bilgic B, Chan K-S, Hedouin R, et al. QSM reconstruction challenge 2.0: A realistic in silico head phantom for MRI data simulation and evaluation of susceptibility mapping procedures. Magn Reson Med. 2021; 86(1):526–42 https://doi.org/10.1002/mrm.28716 PMID: 33638241

97. Beaulieu C. The basis of anisotropic water diffusion in the nervous system - a technical review. NMR Biomed. 2002; 15(7–8):435–55 https://doi.org/10.1002/nbm.782 PMID: 12489094

98. Zhang H, Schneider T, Wheeler-Kingshott CA, Alexander DC. NODDI: Practical in vivo neurite orientation dispersion and density imaging of the human brain. Neuroimage. 2012; 61(4):1000–16 https://doi.org/10.1016/j.neuroimage.2012.03.072 PMID: 22484410

99. Berman JI, Lanza MR, Blaskey L, Edgar JC, Roberts TP. High angular resolution diffusion imaging probabilistic tractography of the auditory radiation. AJNR Am J Neuroradiol. 2013; 34(8):1573–8 https://doi.org/10.3174/ajnr.A3471 PMID: 23493892

100. Suri S, Topiwala A, Mackay CE, Ebmeier KP, Filippini N. Using structural and diffusion magnetic resonance imaging to differentiate the dementias. Curr Neurol Neurosci Rep. 2014; 14(9):475 https://doi.org/10.1007/s11910-014-0475-3 PMID: 25030502

101. Goveas J, O'Dwyer L, Mascalchi M, Cosottini M, Diciotti S, De Santis S, et al. Diffusion-MRI in neurodegenerative disorders. Magn Reson Imaging. 2015; 33(7):853–76 https://doi.org/10.1016/j.mri.2015.04.006 PMID: 25917917

102. Tax CMW, Bastiani M, Veraart J, Garyfallidis E, Okan Irfanoglu M. What's new and what's next in diffusion MRI preprocessing. Neuroimage. 2022; 249:118830 https://doi.org/10.1016/j.neuroimage.2021.118830 PMID: 34965454

103. Tustison NJ, Avants BB, Cook PA, Zheng Y, Egan A, Yushkevich PA, et al. N4ITK: improved N3 bias correction. IEEE Trans Med Imaging. 2010; 29(6):1310–20 https://doi.org/10.1109/TMI.2010.2046908 PMID: 20378467

104. Avants BB, Epstein CL, Grossman M, Gee JC. Symmetric diffeomorphic image registration with cross-correlation: evaluating automated labeling of elderly and neurodegenerative brain. Med Image Anal. 2008; 12(1):26–41 https://doi.org/10.1016/j.media.2007.06.004 PMID: 17659998

105. Billot B, Greve DN, Puonti O, Thielscher A, Van Leemput K, Fischl B, et al. SynthSeg: Segmentation of brain MRI scans of any contrast and resolution without retraining. Medical Image Anal. 2023; 86:102789 https://doi.org/10.1016/j.media.2023.102789 PMID: 36857946

106. Veraart J, Novikov DS, Christiaens D, Ades-Aron B, Sijbers J, Fieremans E. Denoising of diffusion MRI using random matrix theory. Neuroimage. 2016; 142:394–406 https://doi.org/10.1016/j.neuroimage.2016.08.016 PMID: 27523449

107. Tournier JD, Smith R, Raffelt D, Tabbara R, Dhollander T, Pietsch M, et al. MRtrix3: A fast, flexible and open software framework for medical image processing and visualisation. Neuroimage. 2019; 202:116137 https://doi.org/10.1016/j.neuroimage.2019.116137 PMID: 31473352

108. Andersson JLR, Sotiropoulos SN. An integrated approach to correction for off-resonance effects and subject movement in diffusion MR imaging. Neuroimage. 2016; 125:1063–78 https://doi.org/10.1016/j.neuroimage.2015.10.019 PMID: 26481672

109. Yeatman JD, Dougherty RF, Myall NJ, Wandell BA, Feldman HM. Tract Profiles of White Matter Properties: Automating Fiber-Tract Quantification. Plos One. 2012; 7(11):e49790 https://doi.org/10.1371/journal.pone.0049790 PMID: 23166771

110. Kruper J, Yeatman JD, Richie-Halford A, Bloom D, Grotheer M, Caffarra S, et al. Evaluating the reliability of human brain white matter tractometry. Apert Neuro, 2021; 1(1), https://doi.org/10.52294/e6198273-b8e3-4b63-babb-6e6b0da10669 PMID: 35079748

111. Tournier JD, Calamante F, Connelly A, editors. Improved probabilistic streamlines tractography by 2nd order integration over fibre orientation distributions. Proceedings of the international society for magnetic resonance in medicine; 2010: ISMRM.

112. Daducci A, Canales-Rodríguez EJ, Zhang H, Dyrby TB, Alexander DC, Thiran JP. Accelerated Microstructure Imaging via Convex Optimization (AMICO) from diffusion MRI data. Neuroimage. 2015; 105:32–44 https://doi.org/10.1016/j.neuroimage.2014.10.026 PMID: 25462697

113. Smith SM, Fox PT, Miller KL, Glahn DC, Fox PM, Mackay CE, et al. Correspondence of the brain's functional architecture during activation and rest. Proc Natl Acad Sci U S A. 2009; 106(31):13040–5 https://doi.org/10.1073/pnas.0905267106 PMID: 19620724

114. Smith SM, Nichols TE, Vidaurre D, Winkler AM, Behrens TE, Glasser MF, et al. A positive-negative mode of population covariation links brain connectivity, demographics and behavior. Nat Neurosci. 2015; 18(11):1565–7 https://doi.org/10.1038/nn.4125 PMID: 26414616

115. Zhang Y, Brady M, Smith S. Segmentation of brain MR images through a hidden Markov random field model and the expectation-maximization algorithm. Ieee T Med Imaging. 2001; 20(1):45–57 https://doi.org/10.1109/42.906424 PMID: 11293691

116. Andersson JLR, Skare S, Ashburner J. How to correct susceptibility distortions in spin-echo echo-planar images: application to diffusion tensor imaging. Neuroimage. 2003; 20(2):870–88 https://doi.org/10.1016/S1053-8119(03)00336-7 PMID: 14568458

117. Jenkinson M, Bannister P, Brady M, Smith S. Improved optimization for the robust and accurate linear registration and motion correction of brain images. Neuroimage. 2002; 17(2):825–41 https://doi.org/10.1016/s1053-8119(02)91132-8 PMID: 12377157

118. Behzadi Y, Restom K, Liau J, Liu TT. A component based noise correction method (CompCor) for BOLD and perfusion based fMRI. Neuroimage. 2007; 37(1):90–101 https://doi.org/10.1016/j.neuroimage.2007.04.042 PMID: 17560126

119. Pruim RHR, Mennes M, van Rooij D, Llera A, Buitelaar JK, Beckmann CF. ICA-AROMA: A robust ICA-based strategy for removing motion artifacts from fMRI data. Neuroimage. 2015; 112:267–77 https://doi.org/10.1016/j.neuroimage.2015.02.064 PMID: 25770991

120. Vizioli L, Moeller S, Dowdle L, Akcakaya M, De Martino F, Yacoub E, et al. Lowering the thermal noise barrier in functional brain mapping with magnetic resonance imaging. Nat Commun. 2021; 12(1):5181 https://doi.org/10.1038/s41467-021-25431-8 PMID: 34462435

121. Moeller S, Pisharady PK, Ramanna S, Lenglet C, Wu X, Dowdle L, et al. NOise reduction with DIstribution Corrected (NORDIC) PCA in dMRI with complex-valued parameter-free locally low-rank processing. Neuroimage. 2021; 226:117539 https://doi.org/10.1016/j.neuroimage.2020.117539 PMID: 33186723

122. Hendriks J, Mutsaerts HJ, Joules R, Peña-Nogales Ó, Rodrigues PR, Wolz R, et al. A systematic review of (semi-)automatic quality control of T1-weighted MRI scans. Neuroradiology. 2024; 66(1):31–42 https://doi.org/10.1007/s00234-023-03256-0 PMID: 38047983